SEISMIC INTERPRETATION AND STRUCTURAL ANALYSIS OF THE ALLEGHANIAN FOLD-THRUST BELT IN CENTRAL ALABAMA

by

CRAIG LEE CATO

DELORES M. ROBINSON, COMMITTEE CHAIR
ANDREW M. GOODLIFFE
SAMANTHA E. HANSEN
JACK C. PASHIN

A THESIS

Submitted in partial fulfillment of the requirements
for the degree of Master of Science
in the Department of Geological Sciences
in the Graduate School of
The University of Alabama

TUSCALOOSA, ALABAMA

2014

ABSTRACT

In the central part of the Alleghanian fold-thrust belt of Alabama, multi-channel seismic and well log data are used to analyze structural elements of the thrust belt. Six horizons were interpreted on the seismic data in two-way travel time and were depth-converted using interval velocities derived from a synthetic seismogram as well as from sonic logs from USS-29-01-09 and COGC-USX #1. The structural interpretation from the depth-converted data shows the thrust belt is a forward-propagating thrust sequence with four main thrust faults branching off of a basal detachment. Basement along the profile is at a minimum depth of 4,700 m in the Black Warrior Basin and a maximum depth of 7,200 m in the Birmingham Graben System, yielding 2,500 m of relief in this Precambrian rift system. The coherent reflectors in this cross-section show no evidence for a ductile duplex; thus, the section was balanced using line length balancing techniques. The balanced cross-section yields a minimum of 30 km or 24% shortening. This value is similar to other balanced cross-sections to the north and south that span the Alleghanian fold-thrust belt in Alabama.

DEDICATION

“Geology has shared the fate of other infant sciences, in being for a while considered hostile to revealed religion; so like them, when fully understood, it will be found a potent and consistent auxiliary to it, exalting our conviction of the Power, and Wisdom, and Goodness of the Creator.”

-William Buckland

“The most exciting phrase to hear in science, the one that heralds the most discoveries, is not Eureka! (I found it!) but 'That's funny...’”

- Isaac Asimov

This thesis is dedicated to my grandfather, John M. Barnes.

LIST OF ABBREVIATIONS AND SYMBOLS

2-D Two Dimensional

AI Acoustic Impedance

API American Petroleum Institute

BA Birmingham Anticlinorium

BES Belle Ellen Syncline

BCA Blue Creek Anticline

BCS Blue Creek Syncline

BCT Blue Creek Thrust

BGS Birmingham Graben System

BTZ Bessemer Transverse Zone

BWB Black Warrior Basin

CAH Cahaba Synclinorium

CALI Caliper

COO Coosa Synclinorium

DCT Dry Creek Thrust

DPHI Density Porosity

DT Sonic

DST Dickey Springs Thrust

ET Elliotsville Thrust

FM Formation

ft Feet

ft/s Feet per second

GR Gamma Ray

HT Helena Thrust

JVT Jones Valley Fault

LS Limestone

m Meter

m/s Meter per second

Ma Millions of years before present

MMT McAshan Mountain Backthrust

MD Measured Depth

µs/ft Microseconds per foot

OVT Opossum Valley Fault

RC Reflection Coefficient

RHOB Density

s Second

SA Sequatchie Anticline

SCT Spring Creek Thrust

SH Shale

SP Spontaneous Potential

SS Sandstone

SST Shelby Springs Thrust

TA Tacoa Anticline

TCT Talladega-Cartersville Thrust

TD Total Depth

TVD True Vertical Depth

Undiff. Undifferentiated

USS U.S. Steel

ACKNOWLEDGMENTS

This research would not have been possible without the help of so many people through the years. The first acknowledgements go to my thesis committee. My advisor, Dr. Delores Robinson, deserves special recognition for taking me on as a student, for sharing her knowledge of structural geology and tectonics with me, and for working with me to make up for a time when she was on sabbatical. Dr. Andrew Goodliffe helped me extensively with manipulation of seismic data through the entire project and as an advisor for the Imperial Barrel Award competition. Thanks also to Samantha Hansen for her thoughtful edits and timely feedback, as well as for having an open door when I had any questions, and Dr. Jack Pashin for sharing with me his knowledge of Alabama geology. My friends and fellow graduate students also deserve recognition for all of the help they gave me with a number of issues: the Structure group members (Subhadip Mandal, Subodha Khanal, Andrea Gregg, Ian Hunter, and Will Jackson) for helping immensely with issues from structural methods and principles to questions about computer programs, Jordan Graw for his help with GMT, my roommate Jeffrey Madden for always being available for help with any geology-related topics, and to all my friends for making it possible for me to keep my sanity through tremendously stressful times. Thank you to The University of Alabama Department of Geological Sciences for supporting me with a teaching assistantship and for providing funding that enabled me to travel to research conferences. I would also like to thank the Geological Society of America, Alabama Geological Society, The University of Alabama Graduate Student Association and The University of Alabama College of

Arts and Sciences for providing funding for travel to research conferences. Thank you to Neuralog for donating well digitizing software, and to Schlumberger for donating Petrel seismic software to the University of Alabama. Thank you to the faculty at The University of West Georgia, specifically Randy Kath, Tim Chowns, Chris Berg, Curtis Hollabaugh, Brad Deline, and Randa Harris for preparing me for graduate work by sharing their vast collective knowledge of geology and for helping to grow my love for the subject. Lastly, but certainly not least, I would like to acknowledge my parents, Tim and Beth Cato. They have supported me in so many ways over the years and I would not be where I am today without them (I think my Dad has earned that Cadillac).

CONTENTS

ABSTRACT ii

DEDICATION iii

LIST OF ABBREVIATIONS AND SYMBOLS iv

ACKNOWLEDGMENTS vi

LIST OF TABLES x

LIST OF FIGURES xi

LIST OF PLATES xiii

CHAPTER 1: INTRODUCTION 1

CHAPTER 2: REGIONAL GEOLOGY 4

a. TECTONIC HISTORY: ALABAMA 4

b. STRATIGRAPHY 5

i. Precambrian Basement 7

ii. Cambrian Units 7

iii. Cambrian-Ordovician Units 7

iv. Ordovician Units 8

v. Silurian Units 8

vi. Devonian Units 8

vii. Mississippian Units 9

viii. Pennsylvanian Units 14

c. STRUCTURE 14

i. Transverse Zones 15

ii. Structural Domains 16

CHAPTER 3: METHODS 20

a. SEISMIC LINE 21

b. SYNTHETIC SEISMOGRAM 24

c. DEPTH CONVERSION 29

d. CROSS-SECTION METHODS 31

i. Flexural Slip Restoration 31

CHAPTER 4: RESULTS AND INTERPRETATIONS 40

a. WELL INTERPRETATIONS 40

b. SEISMIC INTERPRETATIONS 41

CHAPTER 5: DISCUSSION 46

a. BALANCED CROSS-SECTION 46

b. KINEMATIC DEVELOPMENT OF THE BALANCED CROSS-SECTION 49

c. COMPARISON WITH OTHER INTERPRETATIONS 51

i. Pearce (2002) 52

ii. Bailey (2007) and Robinson et al. (2012) 52

iii. Thomas and Bayona (2005) 55

iv. Brewer (2004) 59

CHAPTER 6: CONCLUSIONS 64

REFERENCES 66

LIST OF TABLES

1. Depths to formation tops.....22

2. Interpretation unit velocities.....30

3. Formation velocities from Pearce (2002), Gates (2006), Bailey (2007) and Rutter (2012).....30

4. Shortening estimates from previous studies along the Alleghanian fold-thrust belt.....63

LIST OF FIGURES

1. Regional geology of the southern and eastern United States ……..2

2. Geologic provinces, major structures, and data distribution in Alabama.....3

3. Generalized stratigraphic column for the Valley and Ridge Province in Alabama including seismic interpretation units…..6

4. DEM showing major structures, structural domains, and well distribution ……..…….....10

5. Stratigraphy for USS 29-01-09 11

6. Stratigraphy for COGC-USX #1.....12

7. Lithology descriptions for well stratigraphy.....13

8. Cross-section illustrating structural domains in Alabama 19

9. Compiled 1:24,000 scale geologic maps within the study area with seismic interpretation units, major structures, structural domains, original seismic geometry and reprojected seismic geometry 23

10. Wavelet parameters for USS 29-01-09 synthetic 27

11. Synthetic seismogram and well-to-seismic tie for USS 29-01-09.....28

12. Uninterpreted Line 691-12 in two-way travel time. Includes original and reprojected geometries 35

13. Velocity model for Line 691-12 36

14. Basic illustration of cross-section balancing.....38

15. Maps showing seismic line and cross-section line locations from Pearce (2002) and Bailey (2007) 39

16. Uninterpreted and interpreted line 691-12 in depth.....43

17. Annotated and unrestored cross-section. 44

18. Restored cross-section 45

19. Cartoon demonstrating the kinematics of the Talladega-Cartersville Fault.....48

20. Cross-section from Pearce (2002).....53

21. Cross-section from Bailey (2007) and Robinson et al. (2012) showing interpretations A and B 54

22. 1:24,000 scale geologic maps showing the locations of cross-section 16 from Thomas and Bayona (2005) and Brewer (2004) 56

23. Cross-section 16 from Thomas and Bayona (2005) 59

24. Interpreted depth sections of Figure 17 showing a potential zone of incoherent reflectors.....60

25. Cross-section B from Brewer (2004).....63

LIST OF PLATES

1. Uninterpreted and Interpreted Seismic Data……..72

CHAPTER 1

INTRODUCTION

The Alleghanian fold-thrust belt in central Alabama is bounded by the Black Warrior Foreland Basin (BWB) to the west and northwest, the Nashville Dome to the north, the Piedmont Province to the southeast, and the Gulf Coastal Plain to the south (Fig. 1). The thrust belt formed during the Pennsylvanian-Permian Alleghanian orogeny and assembly of the supercontinent Pangea (Thomas and Bayona, 2002). Geologic structures in the thrust belt are northeast-striking folds, extensive northwest-verging thrust faults, backthrusts, and southeast-verging folds that are composed of Cambrian through Pennsylvanian carbonate and siliciclastic rocks (Butts, 1926) that formed parallel to the strike of the Appalachian Mountains in weak layers at the interface between Paleozoic sediments and Precambrian crystalline basement (Thomas, 1988; Thomas and Osborne, 1995). Cambrian shale constitutes a weak layer that hosts the regional detachment, while Cambrian-Ordovician carbonate rocks form a regional stiff layer that controls the structural geometry of the individual thrust sheets (Thomas, 1985; Thomas and Bayona, 2005).

VASTAR Resources, Inc. collected fifteen 2-D, multi-channel seismic lines, perpendicular to strike in the Appalachian fold-thrust belt during the late 1970's and early 1980's as part of an Arco/Amoco thrust belt exploration program (Fig. 2). This study uses Line 691-12, which extends from the leading edge of the Alleghanian fold-thrust belt in Jefferson County, Alabama to Shelby County, Alabama in the southeast (see 4 on Fig. 2). Depth conversion and interpretation of this seismic data, using control from 7 well logs, enables development of a

viable and admissible balanced cross-section along the profile that provides insights into the evolution of central Alabama.

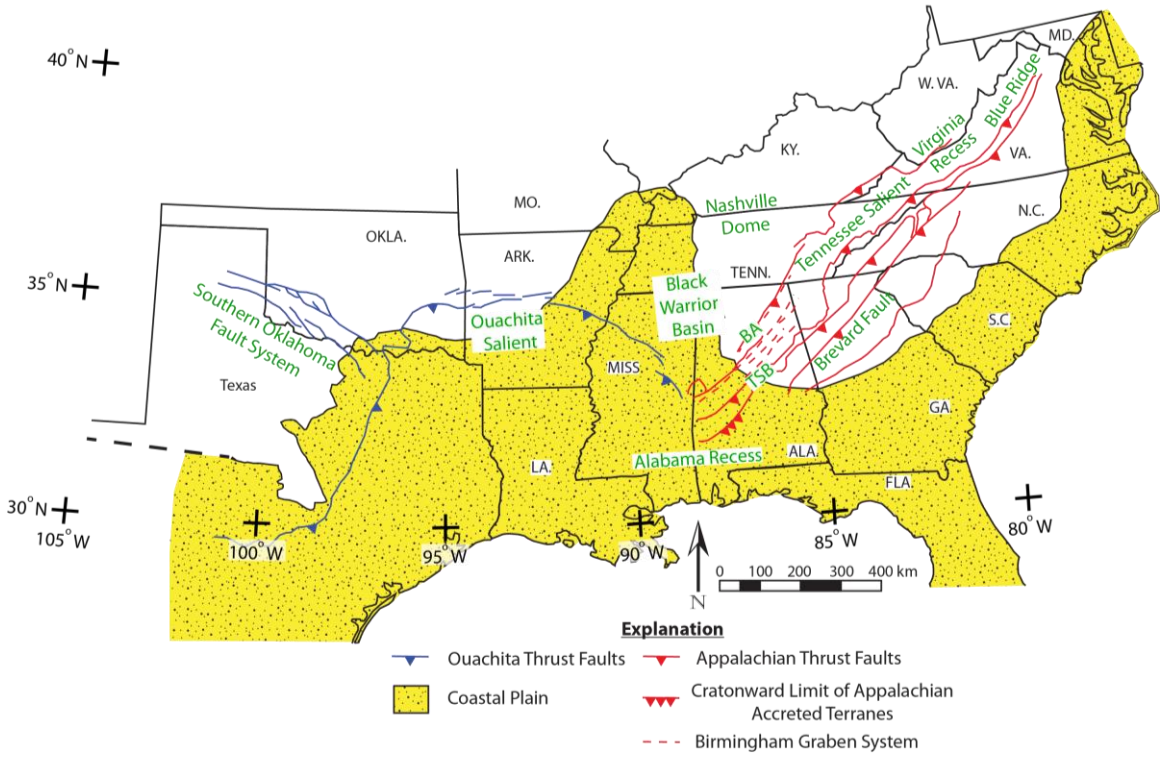

Figure 1. Regional geology of the southeastern United States, including the trends of major structures from the Alleghanian fold-thrust belt, the Ouachita thrust belt, and the extent of Gulf Coastal Plain strata. Green letters represent structure names and abbreviations, while black letters represent state names and abbreviations. BA = Birmingham Anticlinorium, TSB = Talladega Slate Belt. Modified from Thomas (1991) and Thomas et al. (2000).

In Alabama, previous studies with balanced cross-sections of the Alleghanian fold-thrust belt include Gates (2006; 1, Fig. 2), Maher (2002; 2, Fig. 2), Pearce (2002; 3, Fig. 2), Brewer (2004), Thomas and Bayona (2005), and Bailey (2007; 5, Fig. 2), which were focused to the north and south of the current study area in central Alabama. The present study provides a link between research to the north and south by combining geophysical data, structural data, and tectonic concepts and methods. By filling in the gap, I provide an integrated understanding of the Alleghanian fold-thrust belt in Alabama. In addition, determining the evolution of fold-thrust

belts is important for understanding how collisional systems develop and for their value to the oil and gas industry, as thrust systems are commonly targeted for the exploration and production of hydrocarbons.

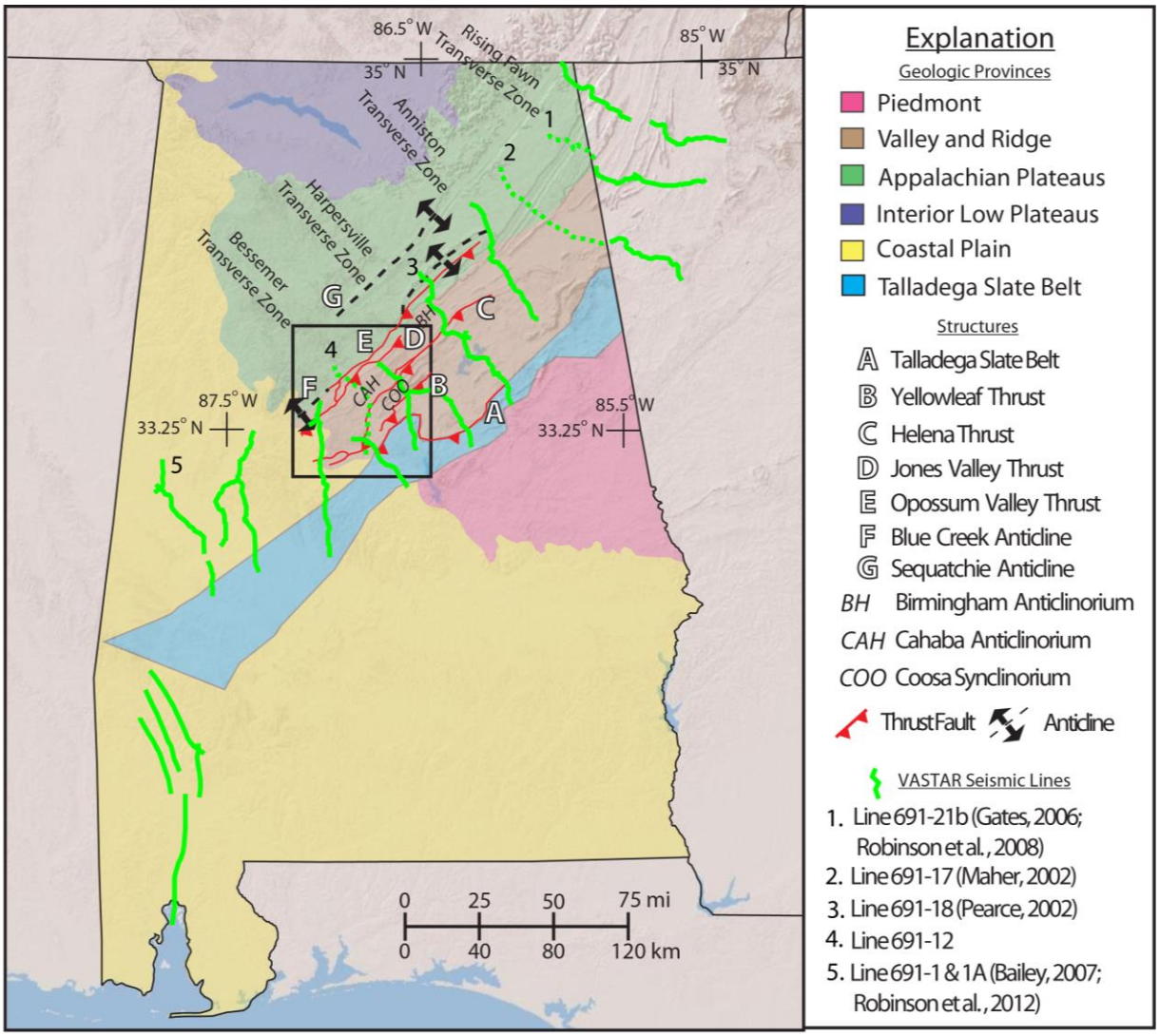

Figure 2. Geologic provinces and major structures in Alabama, including the locations of Transverse Zones. The locations of seismic and well data are also indicated. Solid green lines represent seismic lines from the VASTAR survey; dashed green lines represent sections of lines used in indicated studies (where the entire line was not used). The present study utilizes Line 691-12 (4). Modified from Raymond (1988) and Bailey (2007).

CHAPTER 2

REGIONAL GEOLOGY

TECTONIC HISTORY OF ALABAMA

Rifting began in Late Precambrian to Early Cambrian time along the Blue Ridge Rift, breaking apart the Rodinian supercontinent and forming the Iapetus Ocean (Viele and Thomas, 1989). This episode of rifting also created the Birmingham Graben system (BGS) in central Alabama (Fig. 1). The Blue Ridge Rift defines the eastern margin of Laurentia, which is made-up of six regional salients and six regional recesses (Thomas, 1977; Thomas et al., 2000). A salient occurs where an arcuate thrust belt is convex on the cratonic side, while a recess is concave on the cratonic side (Thomas, 1977). The area of this study lies within the Alabama Recess (Fig. 1). A lack of Late Precambrian synrift rock from Alabama to Texas suggests that the Blue Ridge Rift did not extend south of the BGS (Fig. 1; Thomas et al., 2000). Thomas et al. (2000) report that the Ouachita rift initiated during earliest Cambrian time and that it is represented by synrift igneous rocks in the Southern Oklahoma Aulacogen, synrift sedimentary rocks in the BGS, and the postrift subsidence history of the Laurentian southern margin (Fig. 1). Upward transition from clastic to carbonate rocks indicates that a passive margin developed in central Alabama during Late Cambrian time (510 Ma).

Appalachian orogenesis is the result of successive collisions along the continental margin of eastern North America (Laurentia). The orogen was built by three key events: the Middle Ordovician Taconic Orogeny, the Devonian Acadian Orogeny, and the Late Mississippian-Early

Pennsylvanian Alleghanian Orogeny (Hatcher, 1989). These orogenies represent closure of the Iapetus Ocean. The Taconic Orogeny is the first major compressional event to affect the Laurentian margin as Europe collided with North America. Deformation related to this orogenic event is not present in Alabama. However, sediments related to the event are transported from the north and are present in the Blount clastic wedge, which consists of Middle Ordovician to Middle Silurian deposits (Drake et al., 1989; Brewer, 2004). The Acadian Orogeny may have been caused by an arc-continent collision (Osberg et al., 1989) and may have produced the metamorphism in the Talledega Slate Belt (TSB; Tull, 1982; Osberg et al., 1989). The Alleghanian Orogeny represents the closure of the Paleozoic Iapetus Ocean and the amalgamation of Pangea as Gondwana collided with Laurentia (Hatcher et al., 1989). As the collision progressed, the tectonic and sediment loads from both the Ouachita and Alleghanian Orogens formed the BWB and the southern Appalachians. Synorogenic sediments were shed into the foreland basin (Hatcher et al., 1989). Subsequently, opening of the Gulf of Mexico began at approximately 215 Ma, with extension as Europe and Africa rifted from North America (Thomas, 1989).

STRATIGRAPHY

The Alleghanian fold-thrust belt in Alabama contains Cambrian to Pennsylvanian rocks (Fig. 3) that record the Cambrian rifting of Rodinia (565-535 Ma), subsequent tectonic stability (510 – 340 Ma), and eventual collision (340 Ma) resulting from the Ouachita and Alleghanian Orogenies (Fig. 1; Thomas, 1976; Viele and Thomas, 1989; Pashin, 1994). Thomas (1982) divides the Paleozoic stratigraphy into four parts: (1) basal Cambrian synrift clastic sequence, (2) Cambrian-Ordovician carbonate ramp, (3) Middle Ordovician – Lower Mississippian mixed

carbonate and siliciclastic system, and (4) Mississippian-Pennsylvanian clastic wedge. Figure 3 shows the rock units in central Alabama, both at the surface and in the subsurface.

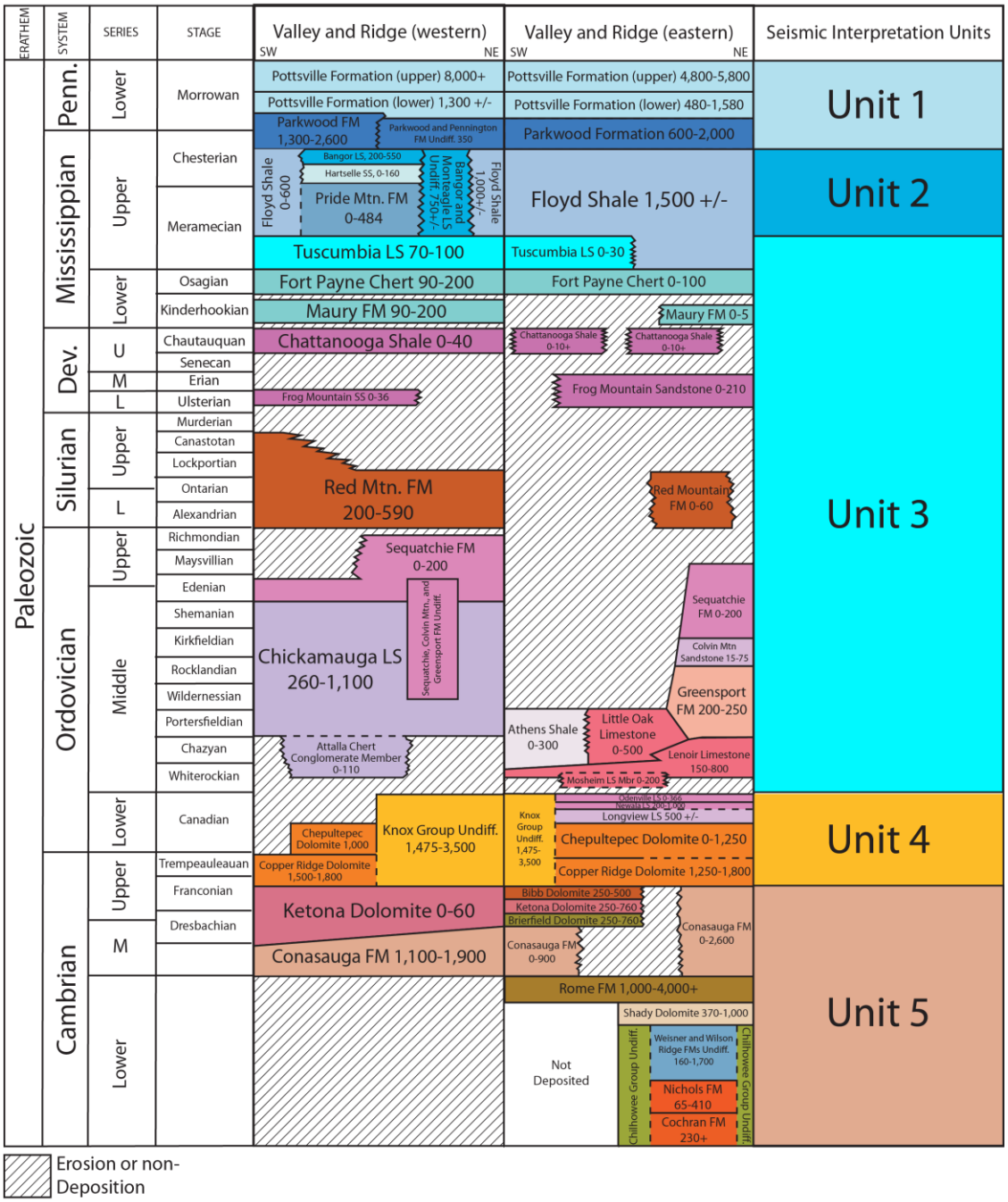

Figure 3**.** Generalized stratigraphy of the Valley and Ridge Province of Alabama with thicknesses in feet. Modified from Szabo et al. (1988). Abbreviations: FM = Formation; Undiff. = undifferentiated; LS = limestone; SS = Sandstone; Mtn. = Mountain.

Precambrian Basement

Paleozoic units in Alabama nonconformably overlie Grenville-age, crystalline basement rocks that range from 750 Ma to 1 Ga (Neathery and Copeland, 1983). Thomas and Bayona (2005) report that the depth to basement of the BGS increases from 2,805 m (9,200 ft) in the NE to approximately 6,100 m (20,000 ft) to the SW. This basement deepening trend is confirmed by seismic and well data south of the present study area (Fig. 2; Bailey, 2007).

Cambrian Units

The Cambrian Rome and Conasauga formations represent an influx of clastic sediment associated with late-stage synrift extension (Thomas, 2007). The Early Cambrian Rome Formation consists of a sequence of red to green shale, mudstone, and sandstone, with occasional carbonate rock and evaporites (Butts, 1926; Raymond et al., 1988). In the fold-thrust belt of Alabama, the Rome Formation can be as thick as 4,000 ft (1,219 m; Raymond et al., 1988; Szabo et al., 1988).

The Middle to Upper Cambrian Conasauga Formation consists of a thick sequence of marine shale and carbonate rock with minor sandstone deposits that record the transition from synrift to passive margin deposition across the Alabama Recess (Raymond et al., 1988; Osborne et al., 2000; Thomas et al., 2000; Thomas and Pashin, 2011; Pashin et al., 2012). In an area that has not been structurally thickened, the Conasauga Formation reaches a thickness of 1,900 ft (579 m; Osborne et al., 2000). The Ketona Dolomite is the carbonate facies equivalent of the Conasauga Formation, consisting of coarse-grained, thickly-bedded dolomite with a maximum thickness of 760 ft (232 m; Raymond et al., 1988).

Cambrian-Ordovician Units

The Knox Group consists of massive carbonate rock deposited on the passive Laurentian platform following Iapetan rifting (Thomas, 2007). The Knox Group is divided into the Odenville Limestone, Newala Limestone, Longview Limestone, Chepultepec Dolomite, and Copper Ridge Dolomite (Raymond et al., 1988). These carbonate rocks are very competent, providing the mechanically stiff layer for the Alleghanian fold-thrust belt. Thomas (2007) reported a maximum thickness in the southern Appalachians of 4,100 ft (1,250 m).

Ordovician Units

The Chickamauga Limestone consists of a sequence of light to dark limestone, shale, and dolomite and is equivalent to the Stones River Group in the BWB (Raymond et al., 1988; Bailey, 2007), with thicknesses ranging from 260-1,100 ft (79-335 m; Raymond et al., 1988). The overlying Sequatchie Formation consists mainly of silty carbonate rock with local fossiliferous limestone and shale interbeds. The thickness ranges from 0-200 ft (0-61 m; Raymond et al., 1988).

Silurian Units

The Silurian Red Mountain Formation consists of shallow marine, dark reddish-brown to olive-gray siltstone, sandstone, and shale with prominent intervals of sedimentary iron (hematite) (Bearce, 1973; Raymond, 1988; Chowns, 2006). It ranges in thickness from 95-590 ft (29-180 m). The hematite beds are between 5-30 ft (1.5-9 m), and provide iron ore to the steel industry in Birmingham.

Devonian Units

The Frog Mountain Sandstone consists of poorly- to well-sorted sandstones interbedded with mudstone. In the lower part of the formation, it contains fossiliferous chert and limestone (Raymond et al., 1988). Thicknesses range from 0-213 ft (0-65 m). The Chattanooga Shale is a

black, carbonaceous, deep-water shale at the top of the Devonian section and, in some locations where the Frog Mountain Sandstone is absent, rests unconformably on Silurian and Ordovician units (Butts, 1926; Raymond, 1988; Pawlewicz and Hatch, 2007; Rheams and Neathery, 1988; Pashin et al., 2010). The thickness of the Chattanooga Shale ranges from 0-90 ft (0-27.5 m; Raymond, 1988; Pashin 2008; Pashin et al., 2010).

Mississippian Units

The Maury Shale consists of 0-7 ft (0-2 m) of greenish-gray to grayish red shale, unconformably overlying Devonian and older rocks (Raymond, 1988; Pashin, 1993). The Fort Payne Chert unconformably overlies the Maury Formation and consists of chert and siliceous microcrystalline limestone (0-207 ft, 0-63 m; Raymond et al., 1988). The upper boundary is a gradational contact with the overlying Tuscumbia Limestone, which consists of 0-250 ft (0-76 m; Raymond et al., 1988) of cherty limestone (Thomas, 1972). The Fort Payne and Tuscumbia are interpreted as a single unit as they possess very similar geophysical characteristics (Bailey, 2007; Fig. 3).

Above the Tuscumbia limestone is the Floyd Shale, which consists primarily of organic-lean, dark-gray marine shale (Raymond et al., 1988; Pashin et al., 2011). The Floyd Shale has a maximum thickness of 2,000 ft (610 m; Raymond et al., 1988), but it is approximately 1,500 ft (457 m) thick in the vicinity of the Coosa synclinorium (Fig, 2; Thomas, 1972; Osborne, 1996). The Floyd Shale is coeval with the Pride Mountain Formation, the Hartselle Sandstone, and the Bangor Limestone (Fig. 3).

The Pride Mountain Formation consists of mostly shale, along with sandstone, oolitic limestone, and shaley limestone, with a maximum thickness of 400 ft (122 m; Thomas, 1972;

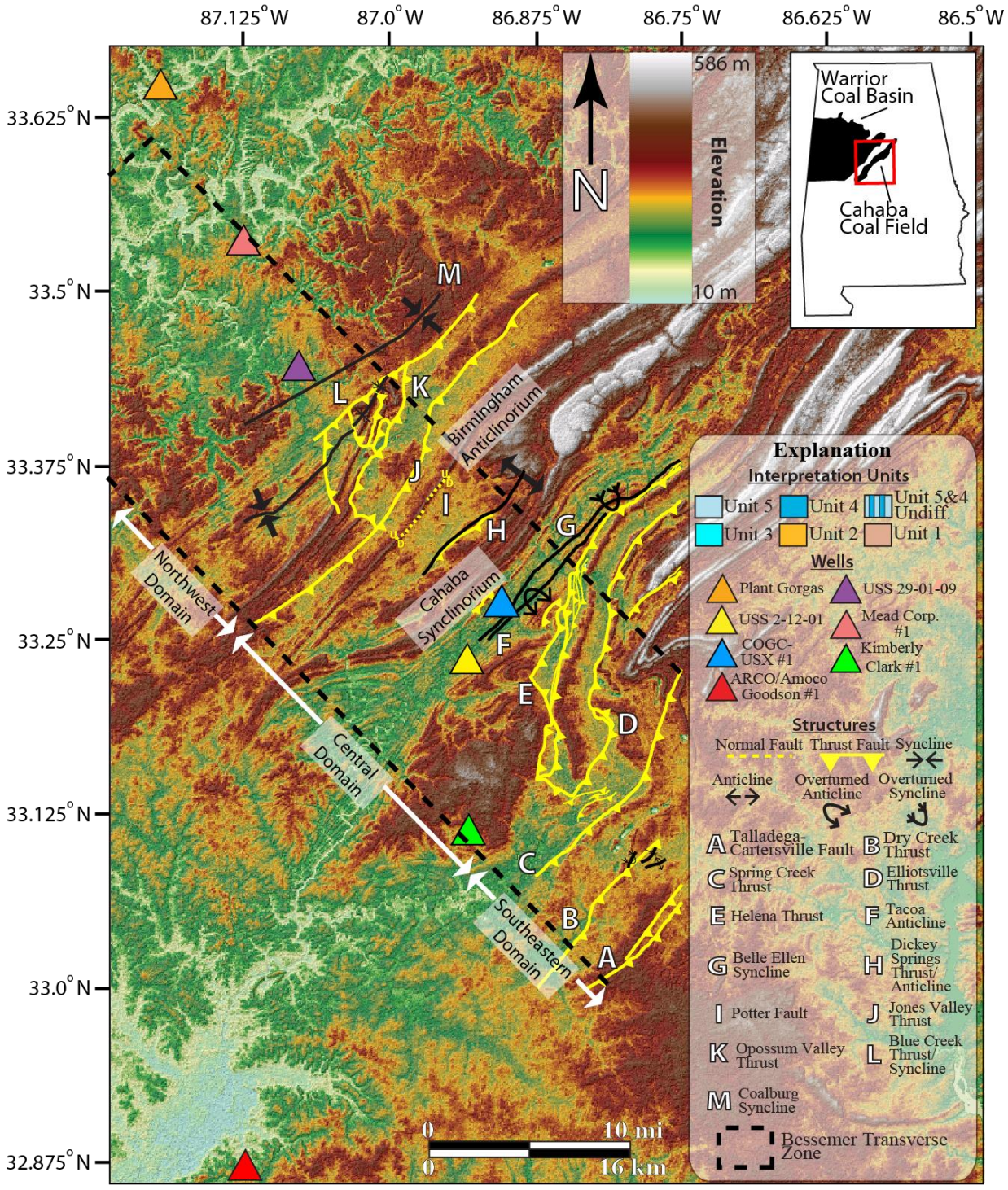

Figure 4. Digital Elevation Model (DEM) of the study area, with the locations of wells, structural domains, and major structures. The dashed black box represents the extent of the Bessemer Transverse Zone.

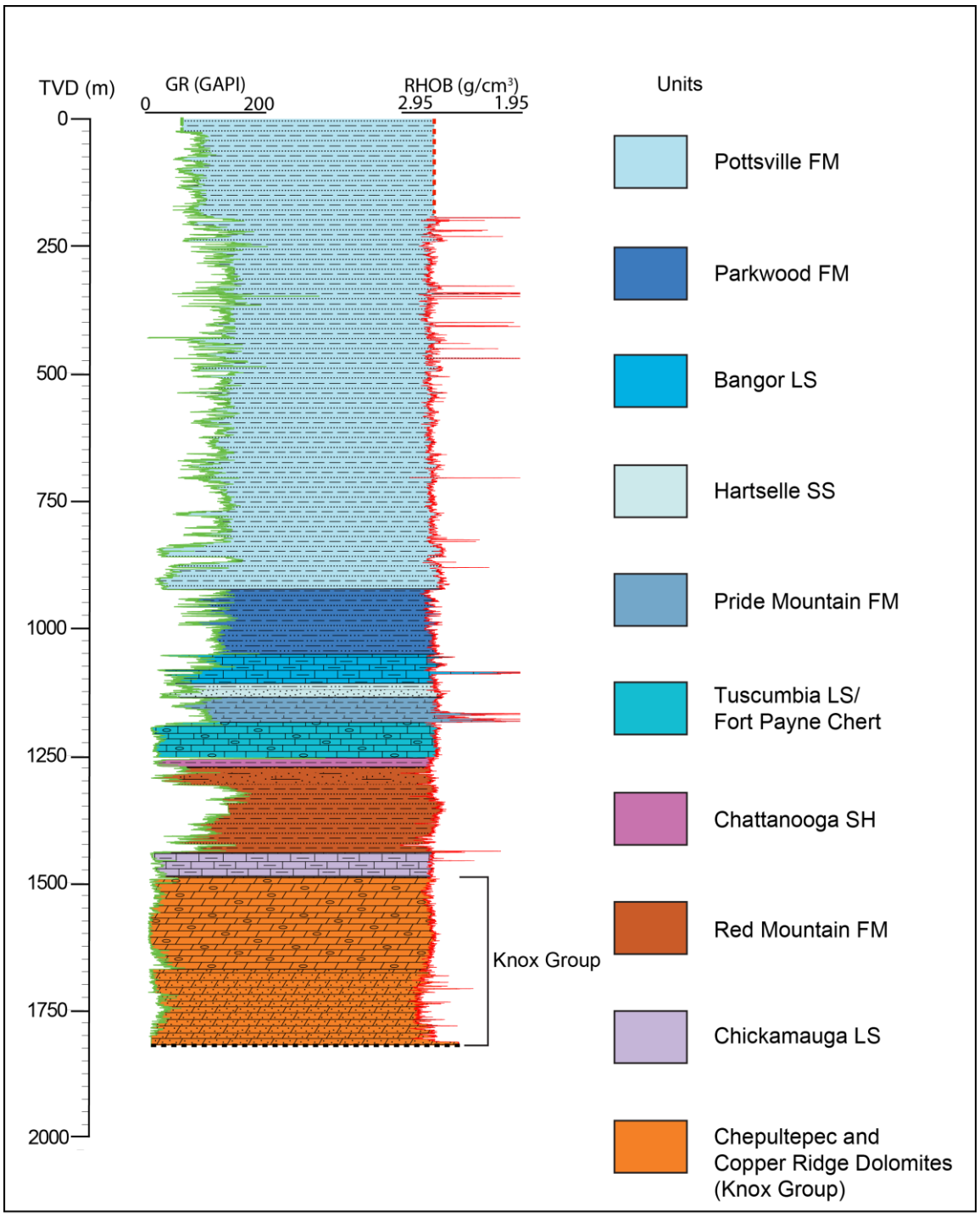

Figure 5. Interpreted stratigraphy from USS 29-01-09. Interpretations are from Pashin et al. (2011). FM=Formation, LS=Limestone, SS=Sandstone. See Figure 7 for lithology descriptions.

Raymond et al., 1988). A disconformity at the base of the Pride Mountain represents the inception of Ouachita orogenesis along the southwestern margin of the Alabama Promontory (Pashin and Rindsberg, 1993a, b).

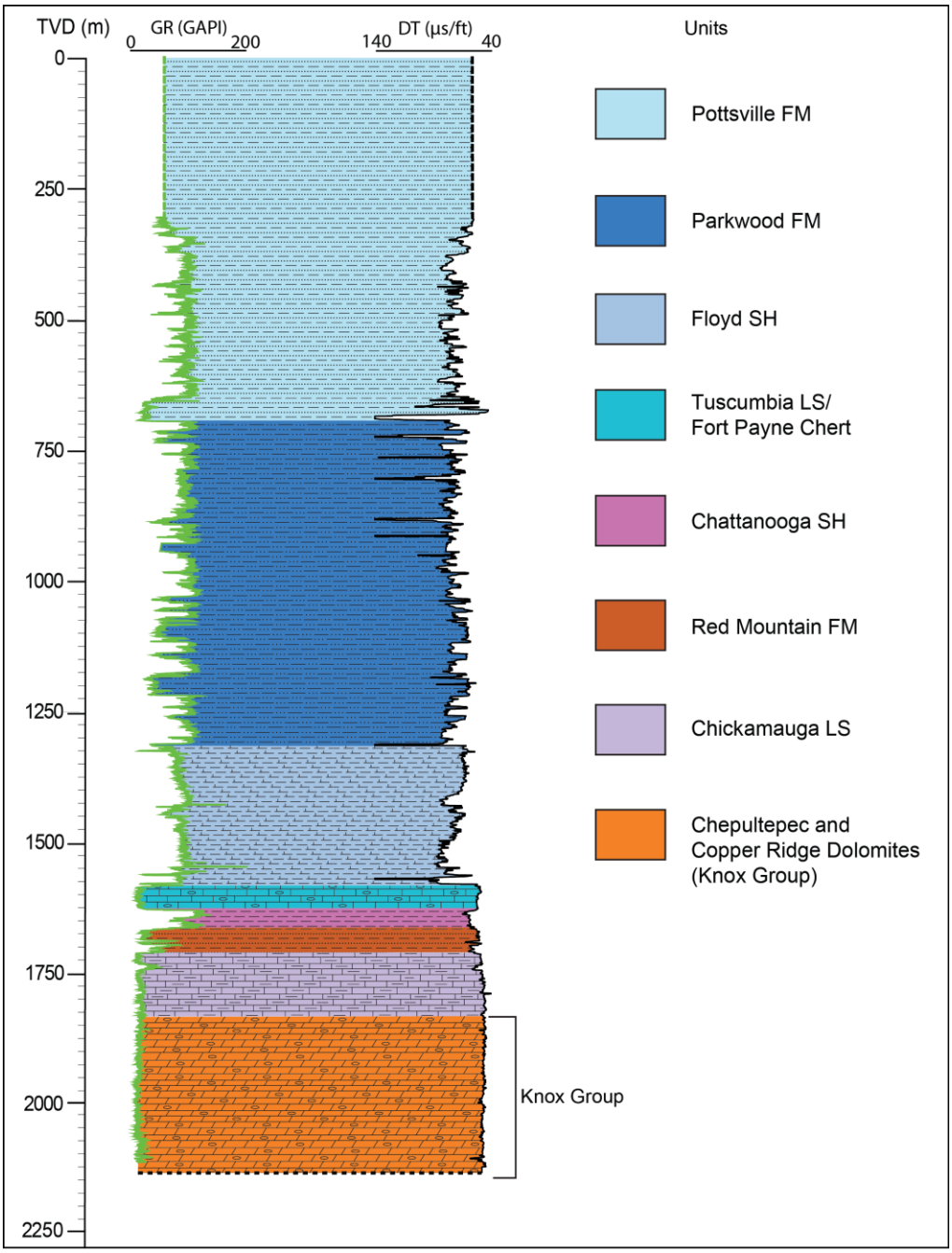

Figure 6. Interpreted stratigraphy from COGC-USX #1. Abbreviations are the same as in Figure 5. See Figure 7 for lithology descriptions.

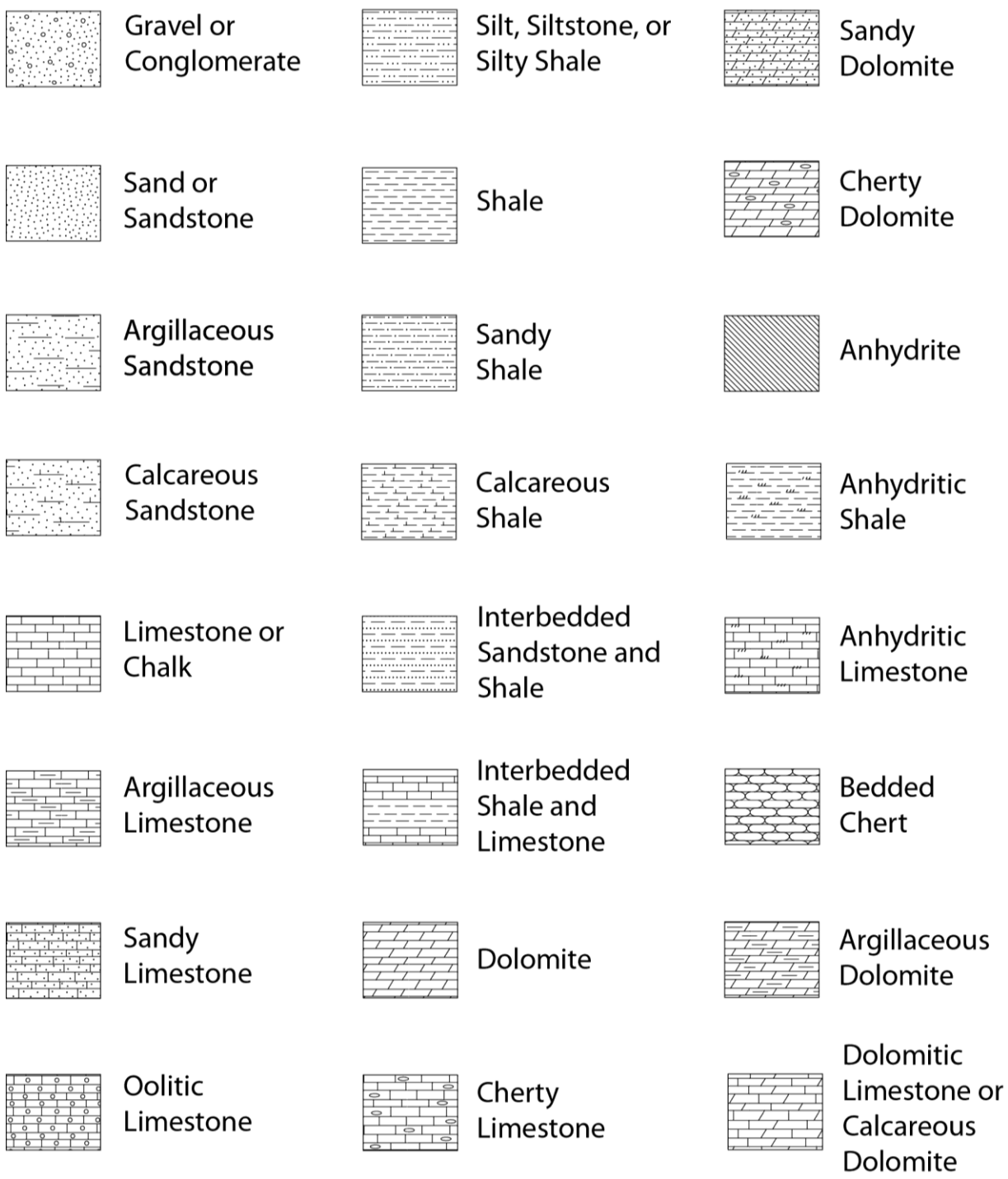

Figure 7. Key for unit lithologies. Descriptions are from Raymond et al. (1988).

The Hartselle Sandstone overlies the Pride Mountain and consists of quartz-arenite sandstone (Thomas, 1972; Thomas and Mack, 1982) with a maximum thickness of 150 ft (46 m; Thomas, 1972; Raymond et al., 1988). The Bangor Limestone is a shallow marine limestone deposited on a carbonate platform that grades into the Floyd Shale to the southwest (Thomas, 1972, 1995; Raymond, 1988). The Bangor Limestone reaches a maximum thickness of approximately 700 ft (214 m; Thomas, 1972; Raymond, 1988).

The Parkwood Formation straddles the boundary between Mississippian and Pennsylvanian time. The Parkwood Formation consists of clay and silt shale with interbeds of sandstone and limestone (Thomas, 1972; Raymond, 1988). The maximum thickness can be as much as 2,500 ft (762 m; Raymond et al., 1988).

Pennsylvanian Units

The Lower Pennsylvanian Pottsville Formation overlies the Parkwood Formation and at the contact there is a quartz-arenite with pebbles (Butts, 1926; Pashin et al., 1995; Pashin and Carroll, 1999). The Pottsville Formation consists of fluvial-deltaic to marginal marine deposits of interbedded shale, siltstone, and coal (Raymond et al., 1988; Pashin, 1991). The Pottsville Formation is composed of sediments shed from the Alleghanian Orogeny (Pashin, 1991, 1993). The thickness of the Pottsville Formation is a maximum of 8500 ft (2,590 m) in the Cahaba coalfield (Raymond et al., 1988; Raymond 1991) and 7,523 ft (2,293 m) in the Kimberley Clark well, where a duplex thickened the unit (Thomas, 1995; Pashin, 2014).

STRUCTURE

The southern Appalachian Mountains in Alabama are characterized by a number of large thrust sheets that are detached at a regional décollement in mechanically weak Cambrian shale and that ramps up section through the Carboniferous clastic wedge (Osborne et al., 2000; Gates,

2006). Under this décollement, basement faults of the BGS are parallel and northeast-striking, with offsets as much 2 km (Thomas, 2004; Thomas and Bayona, 2005). These basement faults also serve as nucleation points for ductile duplexes referred to by Thomas (2001) as "mushwads" (Malleable, Unctuous Shale, Weak-layer Accretion in a Ductile Duplex). Ductile deformation of a thick, mechanically weak layer, such as shale in the Conasauga-Rome interval, generates a ductile duplex structure that elevates and distorts the overlying stiff layer in the Knox Group.

Transverse Zones

Thrust belts are systems of interconnected thrust faults that consist of a three-dimensional system of cross-strike links, including transverse faults, lateral ramps, and zones of displacement transfer (Thomas, 1990; Thomas and Bayona, 2002). Transverse zones are defined as cross-strike alignments of these components and are represented by zones that encompass lateral connectors. They exhibit a range of fault types, different scales of faults, and different senses of apparent offset (Thomas, 1990). Generally, transverse zones are recognized in map view by abrupt along-strike changes in structure, including bending of longitudinal faults, plunging ends of ramp anticlines, and transverse faults (Thomas, 1990; Thomas and Bayona, 2002).

Four transverse zones are present in Alabama (Fig. 2). From northeast to southwest, they are the Rising Fawn transverse zone (RFTZ), the Anniston transverse zone (ATZ), the Harpersville transverse zone (HTZ), and the Bessemer transverse zone (BTZ; Thomas, 1990). The BTZ is located within the study area (Fig. 4; Brewer, 2004). Approximately 10 mi (16 km) wide by 48 mi (77 km) long, the BTZ trends NW-SE and contains NE-striking thrust faults and SW-plunging folds (Brewer, 2004). The distribution of the BTZ at the surface is marked by changes in these structures as they cross the transverse zone, changes in stratigraphic and structural orientations, dip and plunge angles, and displacement of major thrust faults and related

folds (Fig. 4; Szabo et al., 1988; Osborne et al., 1988; Brewer, 2004). Brewer (2004) recognizes seven large-scale thrust faults and numerous minor faults at the surface in the BTZ. The major faults include the Blue Creek (BCT), the Opossum Valley (OVT), the Jones Valley (JVT), the Helena (HT), the Yellowleaf (YT), the Dry Creek (DCT), and the Talladega-Cartersville (TCT). Of the seven thrusts, five exhibit a sinistral change in strike as they cross the BTZ and four terminate in the BTZ, transferring displacement to en-echelon faults across strike (Brewer, 2004). Additionally, several major folds are located in the study area, including the Blue Creek anticline/syncline (BCA/BCS), Birmingham anticlinorium (BA), Cahaba synclinorium (CAH), Coosa synclinorium (COO), Tacoa anticline (TA), and Belle Ellen Syncline (BES). The goal of the current study is to construct a cross-section through the BTZ in order to interpret the geometry of the structures within it and to determine the impact of the structures on tectonic shortening within the BTZ versus other locations along the fold-thrust belt in Alabama.

Structural Domains

Thomas (1982) recognizes three structural domains within the thrust belt in Alabama (Fig. 8): the northwestern domain, central domain, and southeastern domain. The northwestern domain is characterized by narrow, asymmetrical anticlines and broad flat-bottom synclines above a relatively shallow basement, the top of which generally dips at a very gentle 1-2° (Osborne et al., 2000; Bailey, 2007). The Coalburg syncline, BCS, Sequatchie anticline (SA), and BCA are examples of northwestern domain structures. The Sequatchie anticline and Coalburg syncline are located in the footwall of the OVT. The Sequatchie anticline is a fault-bend-fold structure that represents the westernmost extent of Alleghanian deformation, plunging southwest and ending northeast of the Coastal Plain sediments (Thomas and Bearce, 1969; Rutter, 2012; Figs. 2 and 8). The Sequatchie anticline shares its trailing limb with the Coalburg

syncline, which is a footwall-trailing limb ramp underlying the frontal thrust (Brewer, 2004). The BCA is a low amplitude fold and the leading structure of the Alleghanian fold-thrust belt. (Brewer, 2004). The BCA dips into the BCS, a northwest-verging fold in the hanging wall of the BCT that is a fold pair with the BA (Brewer, 2004).

The central domain consists of features between the HT and OVT-JVT, containing several high-relief, fault-related folds and associated frontal thrust ramps as well as a number of northeast-southwest striking normal faults that represent the BGS (Osborne et al., 2000). The HT, BA, CAH, BES, and TA are examples of these structures. The BA and CAH are regional-scale structures with northeast-southwest strikes (Fig. 2). The BA is seated above the northwestern limit of the BGS. Spanning the hanging walls of both the Opossum Valley and Jones Valley thrust sheets, the BA has a steep forelimb, broad, gently-dipping backlimb, and is covered by Coastal Plain sediments to the southwest (Fig. 2; Pashin et al., 1995; Pashin and Carroll, 1999). Thomas (1985b, 1991b) interpretes the BA as a frontal thrust-ramp anticline, while Patterson and Groshong (1989) suggest it is a fault propagation fold. The Cahaba synclinorium is the trailing structure of the Jones Valley thrust sheet and contains a thick package of Paleozoic siliciclastic and carbonate rocks (Pashin et al., 1995; Pashin and Carroll, 1999). The southeastern part of the CAH hosts the Cahaba Coalfield and is bounded to the southeast by the HT, which thrusts Cambrian-Ordovician rocks over Pennsylvanian rocks and dips as much as 70° along the margin of the coalfield (Pashin et al., 1995).

The TA and BES are northeast-striking, northwest-verging map-scale structures located in the southwestern part of the Cahaba Coalfield, in the footwall of the HT (Fig. 4). The TA is an open fold that plunges from < 1° to as much as 10°. The limbs generally dip from 20° to 40°, but

the forelimb can locally exceed 55° (Pashin et al., 1995). The BES is complimentary to the TA, with forelimb dips that range from < 10° to 25° (Pashin et al., 1995).

The southeastern domain contains the geology between the HT and the TCT and is defined by broad, low-angle multiple-level thrust sheets. The HT sheet is the largest example of these thrust sheets (Osborne et al., 2000; Pearce, 2002; Brewer, 2004). The Helena thrust sheet is bounded to the northwest by the HT, which also bounds the trailing limb of the CAH and displays a sinistral change in strike as it crosses the BTZ (Fig. 2 and 4). The HT sheet also includes the YT, Elliotsville thrust, and DCT. Sedimentary rocks of the fold-thrust belt are over-thrust on the southeastern edge of the southeastern domain by the TCT (Fig. 2 and 4), which contains metasedimentary and metavolcanic rocks of greenschist facies of the TSB (Tull, 1982).

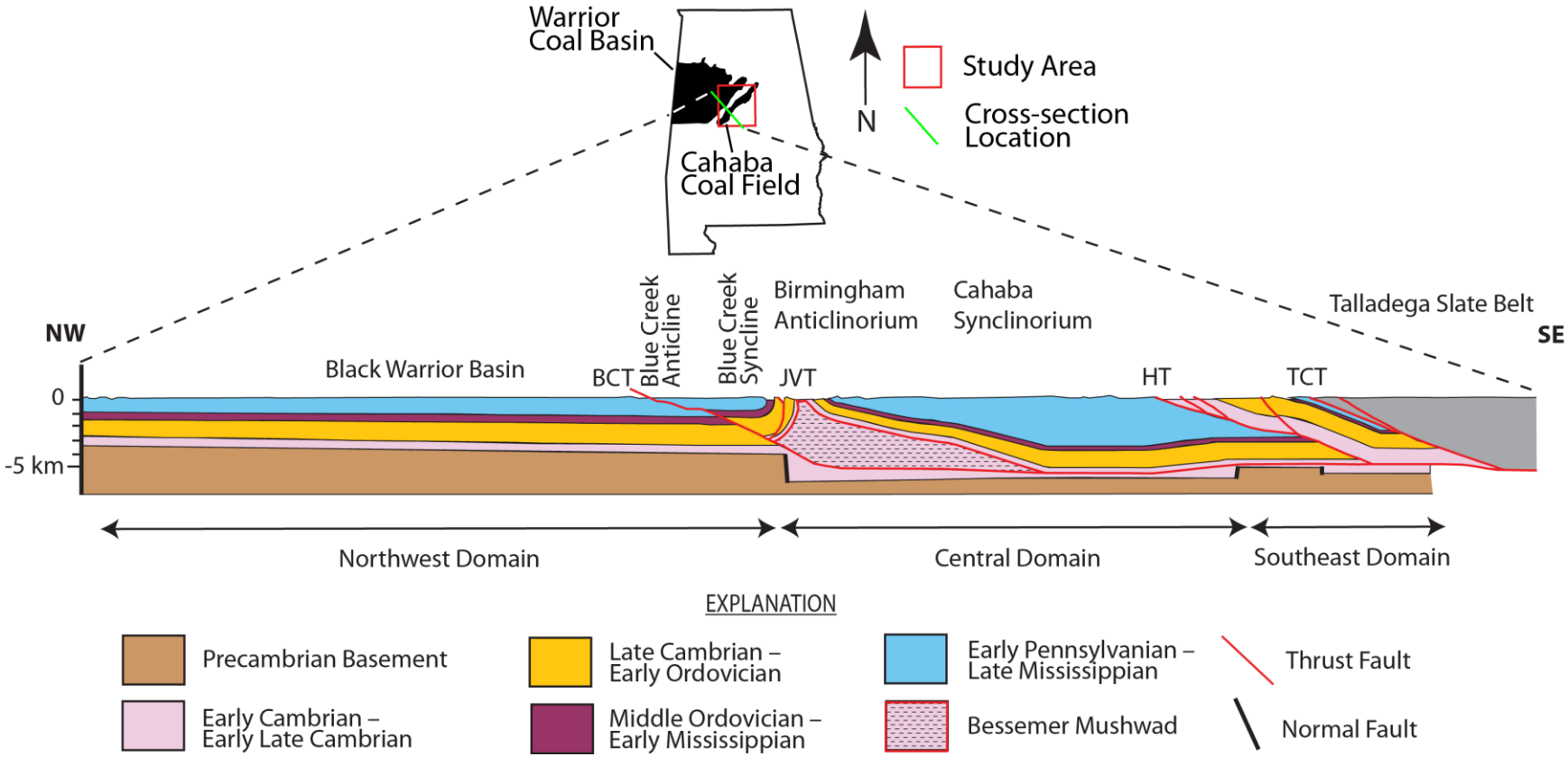

Figure 8. Cross-section showing the three structural domains of the Alleghanian thrust belt in Alabama. Modified from Thomas and Bayona (2005). Scale is 1:1.

CHAPTER 3

METHODS

Given the lack of prominent reflectors, the stratigraphy was grouped into 6 units: 5 sedimentary units and the basement (Fig. 3). Six wells were used for stratigraphic interpretations (Fig. 4): Gorgas #1, Mead Corp. #1 (permit 2260), USS 29-01-09 (permit #12791; Fig. 5), USS 2-12-01 (permit #12943-SWD-03-01), COGC-USX #1 (permit #10082; Fig. 6), and Kimberly Clark (permit #2827). Gorgas #1, Mead #1, and USS 29-01-09 are located in the foreland basin, while USS 2-12-01, COGC-USX #1, and Kimberly Clark are located in the thrust belt (Fig. 4). Table 1 lists unit thicknesses in each of these wells.

The Precambrian basement was identified based on similarities in reflector characteristics to interpretations made by Maher (2002), Pearce (2002), Gates (2006), Bailey (2007), and Rutter (2012). Unit 1 contains the Rome and Conasauga formations, which were grouped together and identified based on comparisons to the same studies as the basement (Unit 1, Fig. 3). Unit 2 is comprised entirely of the Knox Group, which as a whole has a well-documented appearance on the seismic data, with high amplitude reflectors at the top of the formation, underlain by faint to seismically transparent reflectors. However, the individual units that compose the Knox Group possess very similar seismic properties that make them difficult to distinguish individually (Unit 2, Fig. 3). The Tuscumbia Limestone/Ft. Payne is a prominent regional reflector marking the top of Unit 3, which also includes all Lower Mississippian to Middle Ordovician units (Unit 3, Fig. 3). Unit 4 consists of the Upper Mississippian Pride Mountain Formation, Hartselle Sandstone,

Bangor Limestone, and Floyd Shale (Unit 4, Fig. 3). The Bangor Limestone acts as a prominent reflector due to the drastic change in lithology from the overlying clastic rocks. The final unit, Unit 5, includes the Parkwood and Pottsville Formations (Unit 5, Fig. 3), which were grouped together due to a lack of prominent reflectors (Pearce, 2002; Bailey 2007).

SEISMIC LINE

Previous studies in central Alabama were used to determine unit thicknesses, potential fault geometries, and general reflector characteristics (Fig. 2). Pearce (2002) interpreted Line 691-18, a 54-mi (85-km) profile located ~35 mi (56 km) to the northeast of Line 691-12 (Line 3, Fig. 2). Maher (2002) chose Line 691-17, a 62-mi (100-km) profile located ~87 mi (140 km) northeast of Line 691-12 (Line 2, Fig. 2). Gates (2006) interpreted Line 691-21B, a 7.3-mi (24-km) profile located ~ 112 mi (180 km) to the northeast of Line 691-12 (Line 1, Fig. 2), and Bailey (2007) interpreted Lines 691-1 and 691-1A, which are ~77 mi (124 km) to the southwest of Line 691-12 (Line 5, Fig. 2). In addition, Rutter (2012) interpreted two 5-mi (8.05-km) profiles located ~15 mi (28 km) to the northwest of Line 691-12.

Line 691-12 (Line 4, Fig. 2; Line A, Fig. 9) runs from the BWB in Jefferson County (33.5°N, 87°W) southeast into Shelby County, passing through the city of Bessemer. It turns south near the town of Helena and ends in Chilton County, near the intersection of Jefferson, Chilton, and Bibb Counties (33°N, 86.9°W), with a total distance of approximately 36.9 mi (~59 km). A small gap in the data exists near Alabama Highway 269, potentially due to an abrupt change in the direction of the road. Another small gap occurs where the seismic line runs through the town of Montevallo. Six wells and eight 1:24,000 scale geologic maps from the Alabama Geological Survey were utilized to match seismic reflections with rock units. Of the six wells,

five were projected onto the seismic section: Gorgas, Mead Corp. #1, USS 29-01-09, COGC-USX #1, and USS 2-12-01 (Table 1, Fig. 9).

Prior to importing the seismic data into Petrel, shot points from Line 691-12 were re-projected from their original geometry, which were collected on winding roads, to a straight-line geometry. Generic Mapping Tools (GMT) was used to project the shot points onto a

	Gorgas	Mead Corp. #1	USS 29-01-09	COGC-USX 24-16 #1	USS 2-12-01	Kimberley Clark
Pottsville	Surface	Surface	Surface	Surface	Surface	Surface
Parkwood	631	668	923	699	1507.5	2292.5
Floyd				1323	2173.5	3201
Bangor	707	783	1052			
Hartselle	797	850	1122			
Pride Mtn.	824	876	1155.5			
Tuscumbia/ Ft. Payne	880	926	1190.5	1583.5	2519.5	3604
Chattanooga	941	994	1252	1630.5	2582	3660
Red Mountain	952	1034	1264.5	1669	2625.5	
Sequatchie	1057		????			
Stones River	1142					
Chickamauga			1439.5	1715.5	2679	3697
Chepultepec	1221		1493	1840	2807	
Copper Ridge	1372		1671.5		2970	
Conasauga					3253	
Rome						

Explanation

Well TD (m)

Gorgas	1495
Mead Corp #1	1121
USS 29-01-09	1823
COGC-USX 24-16 #1	2114
USS 2-12-01	3536
Kimberley Clark	3810

Seismic Interpretation Units

Unit 5 Unit 3 Unit 1

Unit 4 Unit 2

Time interval penetrated, unit not present in well

Time interval not penetrated by well

Table 1. Depths to the tops of stratigraphic units (meters) and assignment of seismic interpretation units. The azimuth between the Gorgas and Kimberley Clark wells is 157°. Formation tops in the Gorgas well are from Rutter (2012); tops in the USS 29-01-09 well are from Pashin et al. (2011); tops in the Kimberley Clark well above the Floyd Shale are from Thomas (1995). Kimberley Clark is not projected to the seismic line.

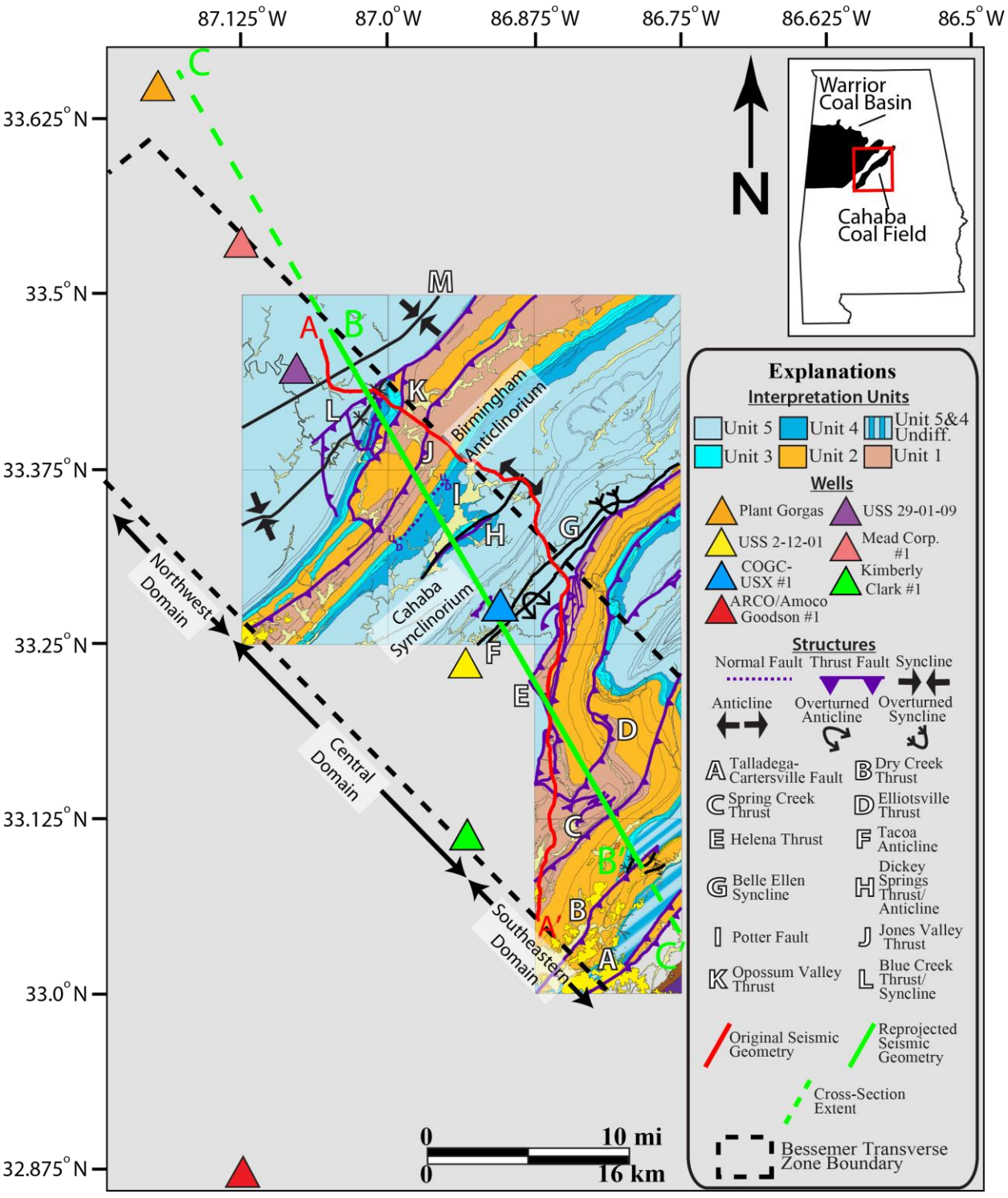

Figure 9. Map consisting of 1:24,000 scale geologic maps compiled from the Alabama Geological Survey, showing the geology in terms of the seismic interpretation units, structural domains, and major structures. The solid red line is the original geometry of Line 691-12, the solid green line is the reprojected geometry of Line 691-12, and the dashed green line represents the endpoints of the cross-section profile.

line centered at 86.9° W longitude and 33.25725° N latitude (Fig. 9). The reprojected profile is approximately 30 mi (48.5 km) in length.

SYNTHETIC SEISMOGRAM

Local stratigraphy and lithology was first defined using mud logs, sample descriptions, and geophysical well log data. The well data was tied to the seismic profile through the use of a synthetic seismogram, or synthetic, which is a modeled seismic reflection response of the earth along a particular borehole, adjusted to give the best match with reflectors in the seismic data (Ewing, 1997). This established a relationship between the well data in depth and the seismic data in time. Formation tops were then assigned to individual reflectors to define the stratigraphy and determine the structural geometry.

Creating a synthetic involved three key steps: (1) calculating acoustic impedance, (2) calculating the reflection coefficient, and (3) convolving the reflection series with a source signal (Bailey, 2007). The acoustic impedance (AI) of a unit is defined as the product of its bulk density and velocity:

$$AI = \rho v$$

where ρ is the bulk density and v is the velocity. In general, the harder a rock is, the higher its AI; the softer a rock, the lower its AI. The contrast in AI between two rock units determines the amount of energy transmitted and reflected at the interface of those units (Kearey et al., 2002). A small contrast represents a higher amount of energy transfer, while a high contrast represents a higher amount of energy being reflected.

The AI contrast can be used to calculate the reflection coefficient, which is a measure of horizon reflectivity (Kearey et al., 2002). It is defined as:

$$R = (AI_2 - AI_1)/ (AI_2 + AI_1)$$

where AI_1 is the acoustic impedance of the first or overlying layer, and AI_2 is the acoustic impedance of the second or underlying layer (Kearey et al., 2002). R is computed for all depth samples, which are then ordered into a set known as a reflectivity series (Kearey et al., 2002). The reflectivity series is then convolved with a wavelet, either idealized or extracted from the seismic data.

Convolution is a mathematical operation that defines the change of shape of a waveform resulting from its passage through a filter (Kearey et al., 2002). The seismogram (filtered output) differs significantly from the initial source (input) due to filtering effects in the ground and those associated with the recording system. The filter effect is defined as:

$$y(t) = g(t) * f(t)$$

where g(t) is the input signal, f(t) is the impulse response, and y(t) is the filtered output. The asterisk denotes the convolution operation (Kearey et al., 2002). When g(t) is the selected wavelet and f(t) is the selected reflectivity series, y(t) is the synthetic trace.

Paper logs from the US Steel 29-01-09 well were digitized to create a synthetic needed for the depth conversion of Line 691-12. The well contained a complete DT log and nearly complete caliper log. While a RHOB log was not available, a DPHI log was available, from which RHOB can be calculated with the following formula:

$$\rho_b = \rho_{ma} - \phi_D(\rho_{ma} - \rho_f)$$

In this equation, ρ_b is bulk density, ρ_{ma} is the matrix density, ϕ_D is DPHI, and ρ_f is fluid density (Asquith and Krygowski, 2004). The ρ_{ma} measurement is 2,710 kg/m^3, obtained from well log headers, and ρ_f is set as 1,000 kg/m^3, the density of water. The sonic curve was converted to velocity by inverting the values and converting them to meters per second (m/s).

Formation tops were picked, establishing formation thicknesses, for which average velocities were calculated. The thickness of a formation was then divided by the average velocity of that formation to determine the amount of time spent in that formation. The same calculation was made for each formation, and the times were progressively summed, establishing a relationship between the depth of a formation and the one-way travel time to the top of that layer. Sonic velocities for the first 200 m were discarded due to casing being set. The synthetic was then projected approximately 1.52 mi (2.45 km) at an azimuth of approximately 090° to trace 41 near the northwest end of the 691-12 seismic line (note: the traces count from 1 to 1146 from northwest to southeast, respectively).

For the US Steel 29-01-09 well, a wavelet was extracted from the seismic data for 40 traces, centered at about trace 41 (Fig. 10). The wavelet was then convolved with the reflectivity series, producing the raw synthetic. After the convolution process, a synthetic must then be adjusted manually relative to high confidence points. The Bangor Limestone, Tuscumbia Limestone, Knox Group, and Conasauga Formation have characteristic seismic signatures known from Pearce (2002), Bailey (2007), Groshong et al. (2010), and Rutter (2012) and as such are viable tie-points. After considering an interpretation of the US Steel 29-01-09 well from Pashin et al. (2011), the top of the Knox Group did not exhibit a distinctive contrast, and the well did not penetrate the Conasauga Formation. Therefore, the Bangor and Tuscumbia Limestones were chosen for the ties (Table 1). After pinning the synthetic at these units, the synthetic was stretched and squeezed to produce a calibrated synthetic used to correlate the well responses with the seismic reflections (Fig. 11). The Bangor was shifted approximately -53.5 ms (in one-way travel time) while the Tuscumbia was shifted -52 ms. This results in an approximately 5% decrease in the difference between the two units, from approximately 28.5 ms prior to adjustment

to 27 ms following adjustment. In addition to well correlations, formation contacts from 1:24,000 scale geologic maps were correlated to the seismic profile to establish a relationship between the surface geology and the subsurface data.

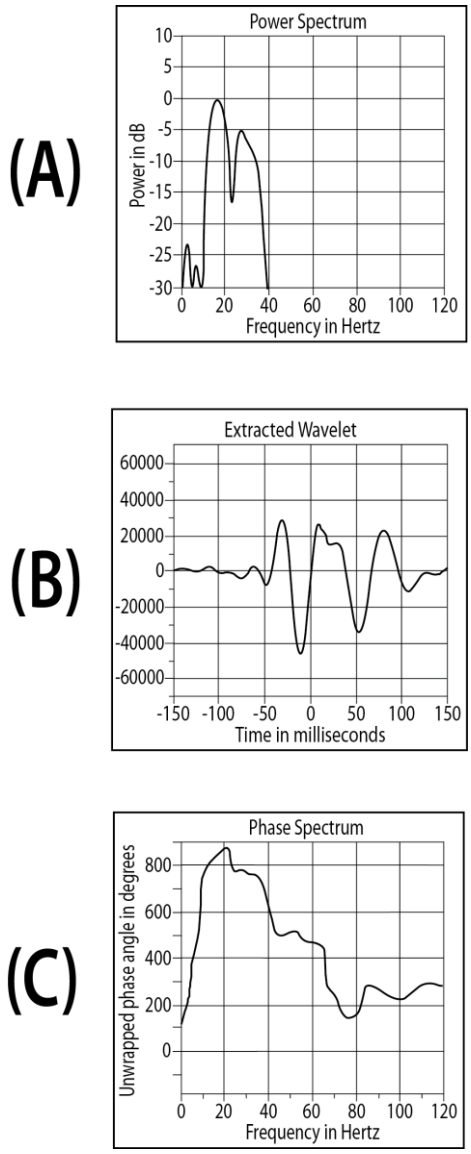

Figure 10. Parameters for the wavelet used in construction of the synthetic for USS 29-01-09. (A) Power in decibels (dB) of the signal across a frequency spectrum in Hertz. (B**)** Wavelet extracted from the seismic data, showing amplitude of the function versus time in milliseconds. (C) Wavelet phase, or initial angle of the function, across a frequency spectrum in Hertz.

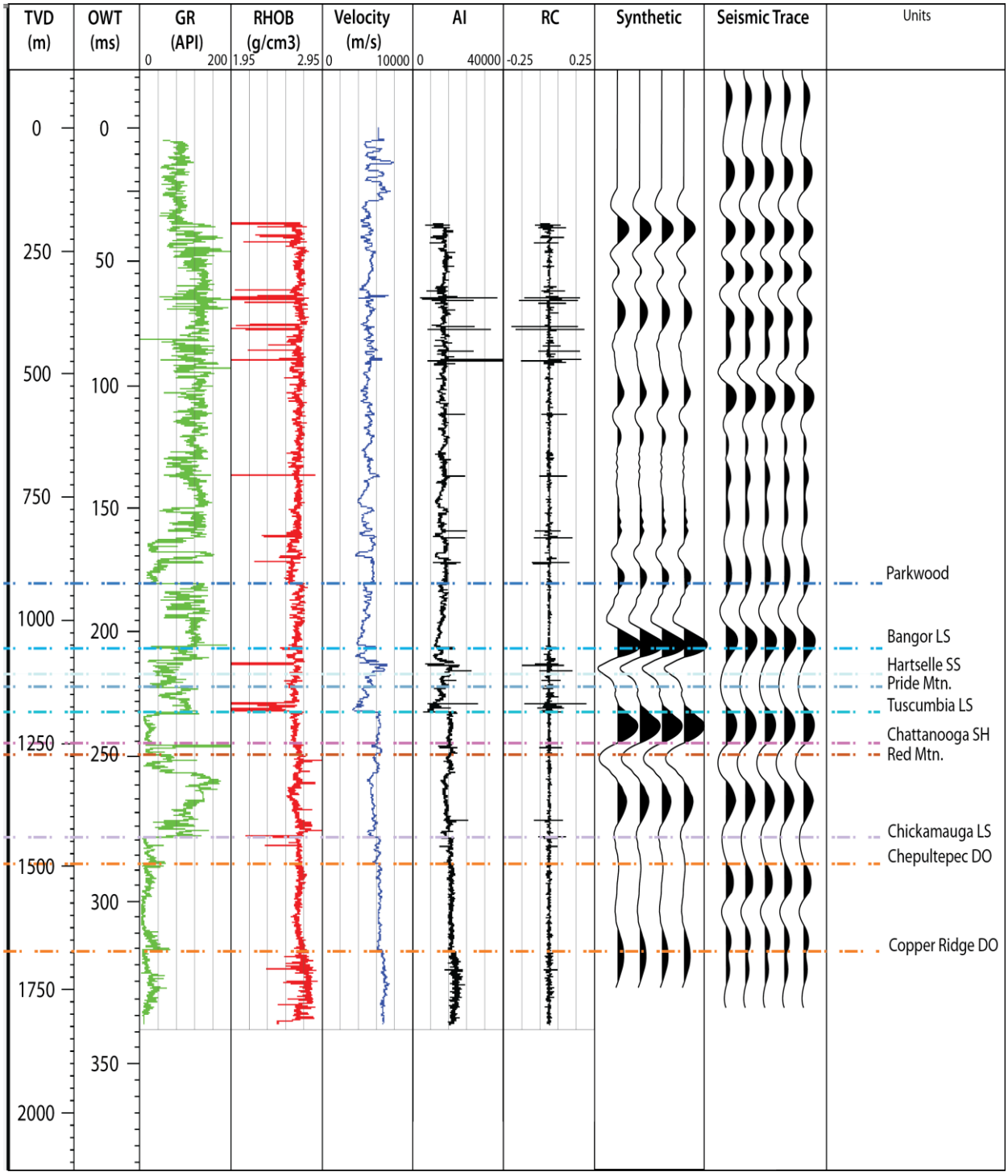

Figure 11. Synthetic seismogram and well-to-seismic tie for USS 29-01-09.

DEPTH CONVERSION

The seismic and well interpretations and depth conversion were carried out using Schlumberger's Petrel E&P software platform. Formation tops were first interpreted on well logs to establish individual thicknesses and velocity characteristics of the formation boundaries, which in turn allowed for construction of the synthetic seismogram (Fig. 11). Table 1 defines the thicknesses for individual formations in each well and the thicknesses for interpretation units.

To make a structural interpretation, the seismic data must be converted from travel-time to depth by constructing a velocity model. Units were first interpreted on the time section and interval velocities were applied to those units. Velocities were calculated using the sonic logs from USS 29-01-09 and COGC-USX #1 (Table 2). COGC-USX #1 was used to account for changes in lithology found within some units, particularly Unit 4, which grades from carbonate rock in the northwest to clastic rock in the southeast (see Stratigraphy, Mississippian Units). The interval velocities were calculated by converting the sonic log from microseconds per foot (μs/ft) to m/s. For USS 29-01-09, interval velocities are: Unit 5 = 4,153 m/s, Unit 4 = 5,121 m/s, Unit 3 = 5,855 m/s, and Unit 2 = 6,524 m/s (Table 2a). From COGC-USX #1, which penetrated the same interpretation units, the velocities are: Unit 5 = 4,256 m/s, Unit 4 = 4,286 m/s, Unit 3 = 6,031 m/s, and Unit 2 = 6,504 m/s (Table 2b). Velocities from both wells were compared to velocities used in similar studies in Alabama (Table 3). Neither USS 29-01-09 nor COGC-USX #1 penetrated Unit 1 or basement. However, velocities of 5,948 m/s and 7,200 m/s, respectively, were assigned based on the work of Pearce (2002). The velocities derived from USS 29-01-09 were used for units northwest of the thrust fault at SP 477 (Figs. 12 and 13). Velocities from COGC-USX #1 were used for units to the southeast of the same structure.

a.

Seismic Unit	Low Velocity	High Velocity	Average Velocity
Unit 5	3119	5800	4153
Unit 4	3257	6558	5130
Unit 3	4853	6570	5850
Unit 2	5288	7409	6583

b.

Seismic Unit	Low Velocity	High Velocity	Average Velocity
Unit 5	1333	7173	4256
Unit 4	2136	5863	4286
Unit 3	4853	7584	6039
Unit 2	5257	6929	6500

Table 2. Velocity ranges and average velocities for seismic interpretation units from (a) USS 29-01-09 and (b) COGC-USX #1. Velocities are in m/s.

A. Pearce (2002)

Unit	Velocity (m/s)
Mississippian-Pennsylvanian	5151
Upper Ordovician -Devonian	5361
Knox Group	6131
Conasauga	5355
Rome and Chilhowee Clastics	5948

B. Gates (2006)

Unit	Velocity (m/s)
Mississippian-Pennsylvanian	4420
Mississippian	5850
Devonian/ Silurian/ Ordovician	4940
Knox Group	6250
Cambrian	5120
Precambrian Basement	6560

C. Bailey (2007)

Unit	Velocity (m/s)
Cretaceous	2025
Mississippian-Pennsylvanian	4557
Devonian/ Silurian/ Ordovician	4757
Chickamauga	6266
Knox Group	6703
Cambrian Dolomite	6995
Cambrian Clastics	5948
Precambrian Basement	7200

D. Rutter (2012)

Unit	Velocity (m/s)
Parkwood	3763
Bangor Limestone	4715
Hartselle Sandstone	5419
Tuscumbia Limestone	4146
Lower Red Mountain	5511
Sequatchie	5091
Conasauga	6300

Table 3. Interval velocities used to convert seismic data to depth from (A) Pearce (2002), (B) Gates (2006), (C) Bailey (2007), and (D) Rutter (2012).

CROSS-SECTION METHODS

The USS 29-01-09 well was projected 1.52 mi (2.45 km) to trace 41 near the northwest end of Line 691-12 (Fig. 9). The projection is used to constrain the tops of interpretation Units 2-5. Although Unit 1 and basement were not penetrated by the well, prominent reflectors were observed in the seismic data, establishing the thickness of Unit 1. Additionally, Gorgas, Mead Corp #1, COGC-USX #1, and USS 2-12-01 were used to constrain depths to formation tops along the cross-section (Table 1). The locations of faults in the seismic data were determined by combining the locations of the faults on geologic maps with the termination of reflectors on the seismic section. Additionally, basement normal faults were interpreted in the seismic data and included in the cross-section.

To validate the depth conversion, a balanced, retro-deformable cross-section must be produced. Balanced cross-sections have their origins in the petroleum industry and were developed in the Canadian Rockies during the 1950's and 1960's to fill in gaps in data. Seismic data acquisition and processing techniques from this period were much less advanced than what is used today, which generally led to lower-quality data (Woodward et al., 1989). Exploration geologists were often only able to distinguish seismic events that correlated to basement. When coupled with the surface geology, this established only two boundaries and left substantial room for ambiguity within the "empty space" in between (Woodward et al., 1983). Dahlstrom (1969) was the first to discuss a detailed outline of the balancing techniques used to test the validity of interpretations made to fill such space.

Flexural Slip Restoration

The flexural slip restoration method is the most suitable to apply in a compressional setting (Woodward, 1989). This method, also referred to as constant bed length and thickness,

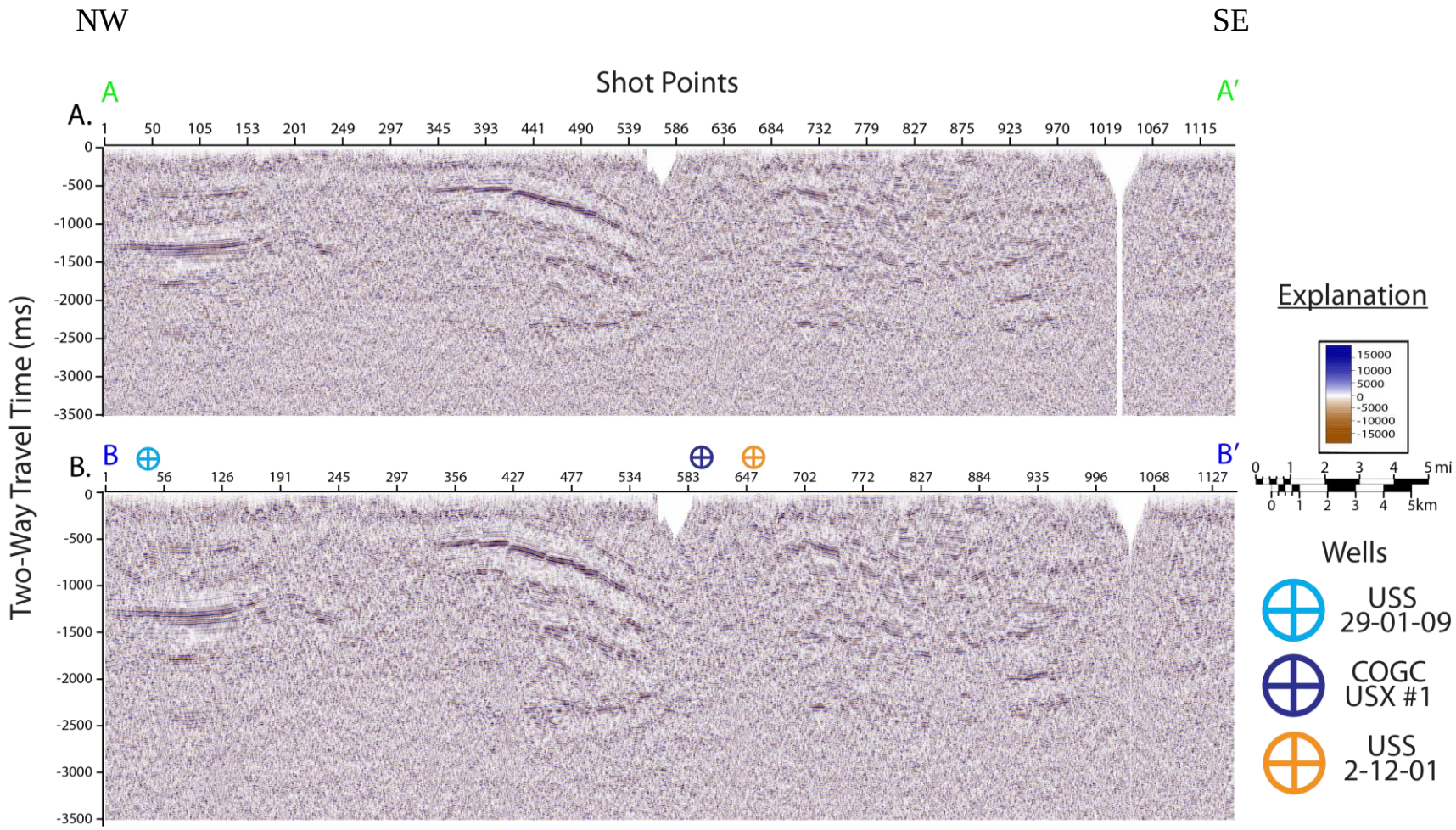

Figure 12. Uninterpreted time section of Line 691-12. (A) Original geometry and (B) reprojected geometry.

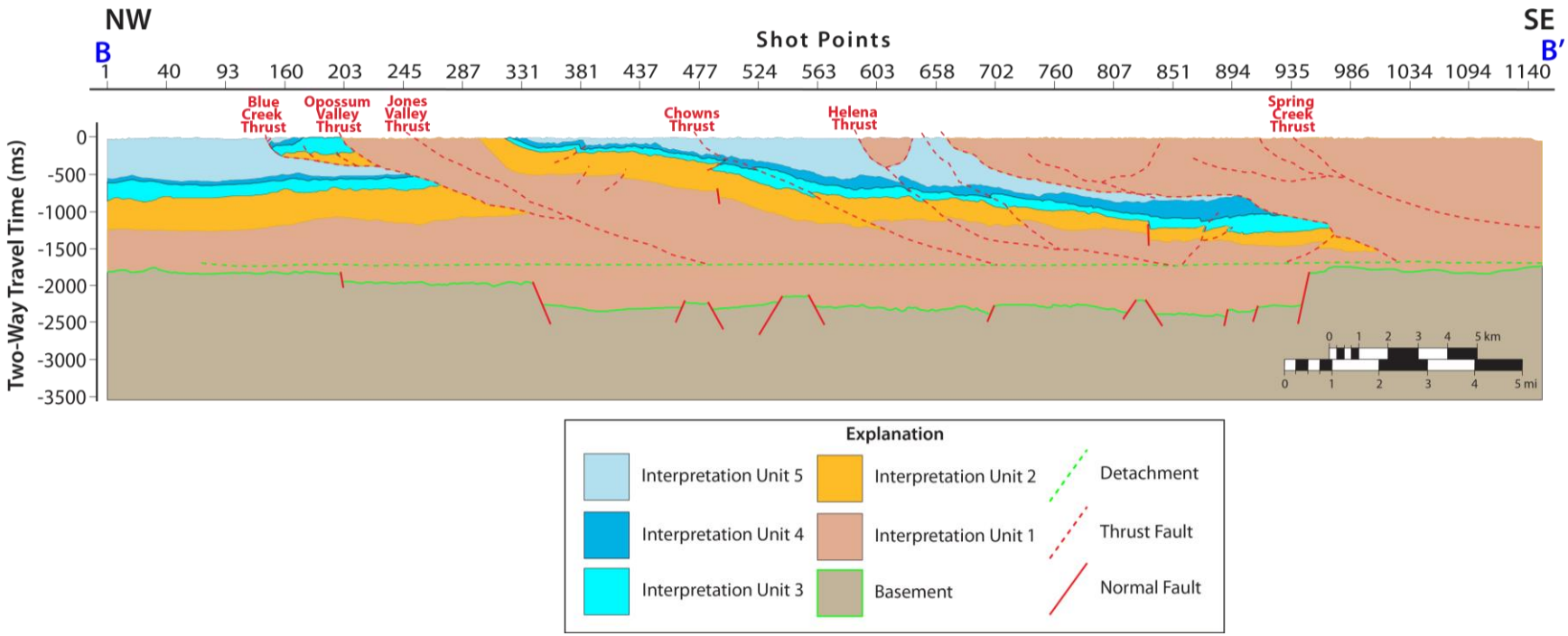

Figure 13. Velocity model for Line 691-12. See Table 2 for velocities assigned to interpretation units.

assumes that slip between coherent beds is parallel (Pearce, 2002). The lengths of interpreted, unrestored horizons are measured in order to restore the horizons to their undeformed state. If a fault is present, the hanging wall and footwall cut-off angles must match (Fig. 14). In a thrust belt setting, the restoration allows for an estimation of shortening due to compression with the following equation:

$$\ell_i - \ell_f = \ell_s$$

$$(\ell_s / \ell_i) \text{ x } 100 = \% \text{ shortening}$$

where ℓ_i represents the length of section prior to compression, ℓ_f represents the length of section after compression, and ℓ_s represents the length of shortening represented in the section.

In a thrust belt, a pin line is selected in the foreland, where slip between the beds equals zero, and it is extended to depth (Fig. 14). This pin line may be anchored by a well or by seismic data, and it is the point from which the lengths of the beds are redrawn. Pin lines were placed at Plant Gorgas and Mead Corp. #1 in the BWB (Figs. 4 and 9). The deepest well, Plant Gorgas, only penetrated to the top of Unit 2. However, Rutter (2012) establishes a depth to the top of Unit 1 of approximately 9,252 ft (2,820 m) from seismic data. Mead Corp #1 penetrated the top of Unit 3 at approximately 3,038 ft (926 m), and the units were projected between the two.

In Pearce (2002) and Bailey (2007), the seismic data were re-projected to straight-line geometry, interpreted, and restored. In those studies, however, the road that the seismic data was recorded along did not display much deviation from the overall trend of the cross-section and as such, the seismic data more closely reflected the subsurface along the entire cross-section (Fig. 15). Line 691-12 was collected on a road that deviates significantly from the path of the cross-section, by as much as 9 mi (14.5 km). Thus, re-projecting the data into a straight line means that the subsurface in the central part of the seismic line may not accurately represent the subsurface

on the cross-section (Fig. 9). To help with the subsurface geology, geologic maps were used to project the faults into the subsurface. Thus, the seismic profile is not balanced; instead, a cross-section line following the path of the re-projected seismic line and extending from the Gorgas well in the northwest to the TCT in the southeast is balanced (Fig. 9). When the seismic line and cross-section line are close to each other, toward the northwest, the seismic interpretation guided the subsurface cross-section geometry in conjunction with the surface geology from the geologic maps (Fig. 9). When the seismic line and cross-section deviated from one another, only geologic maps were used.

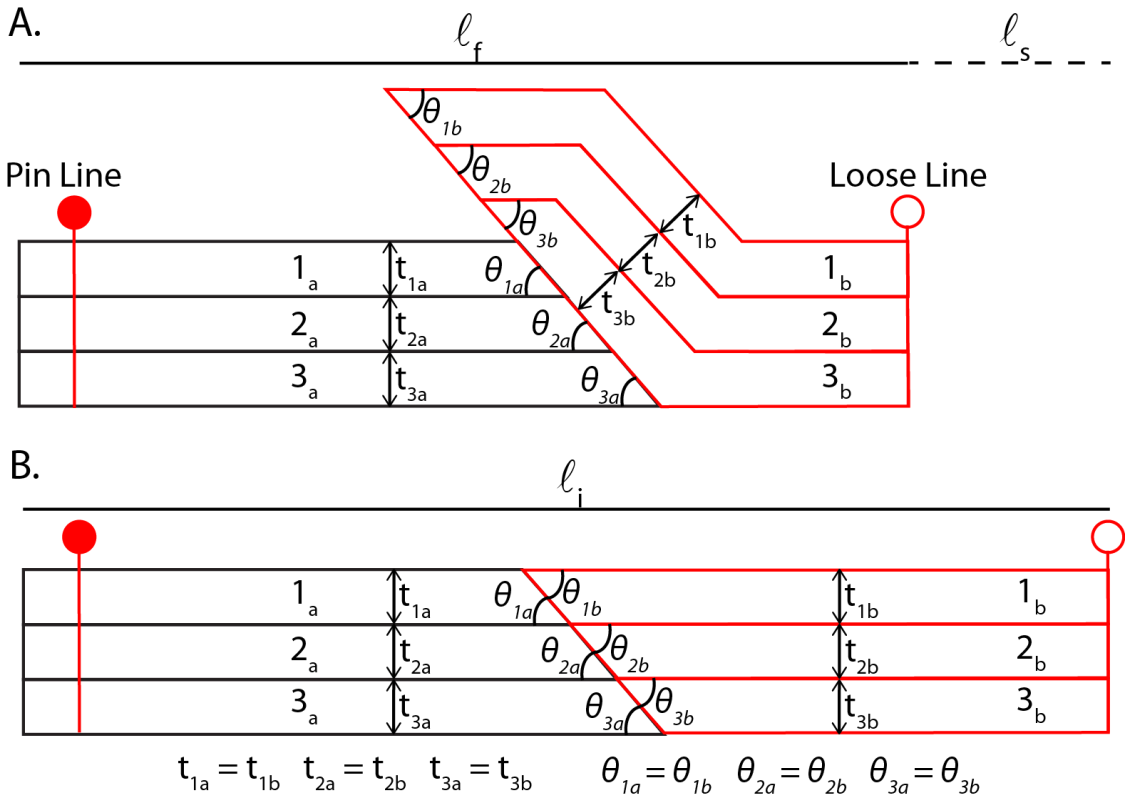

Figure 14. Basic cross-section, demonstrating the process of balancing and restoration. θ represents cut-off angles. ℓ_f represent the final length of the section after shortening, ℓ_i represents the length of the section prior to shortening, and ℓ_s represents the length of shortening in the section.

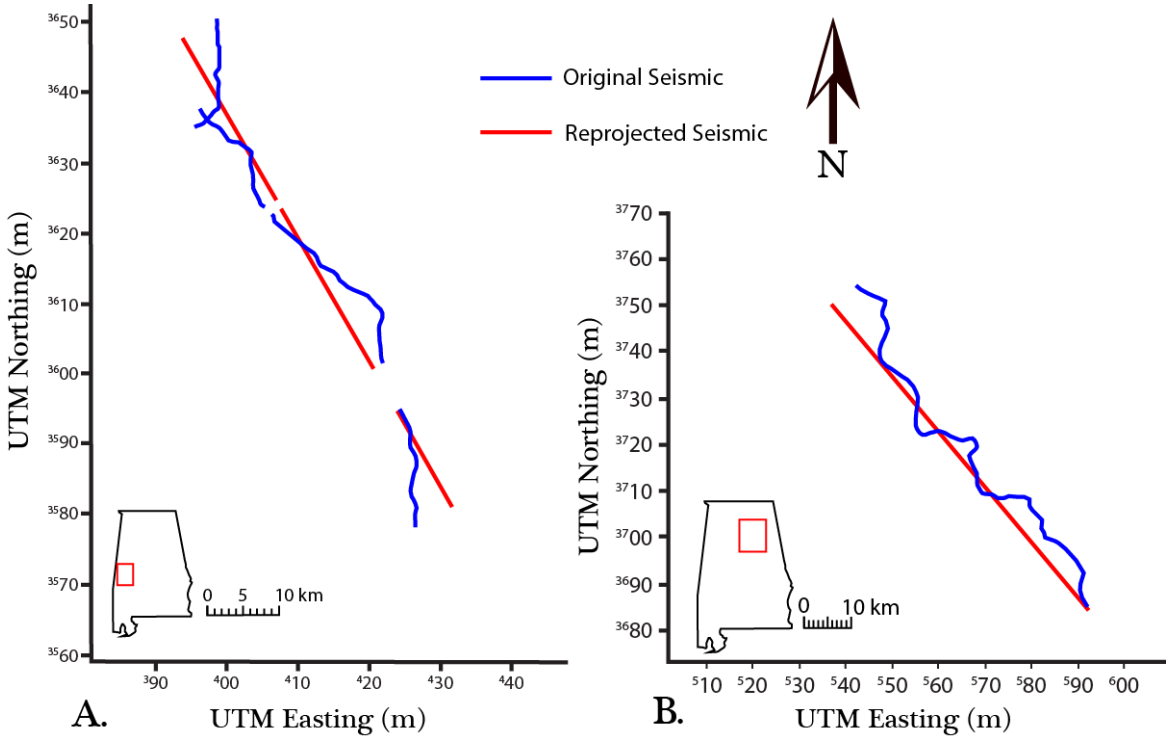

Figure 15. Graphs showing the geometries of the original seismic data and re-projected seismic data from (A) Bailey (2007) and (B) Pearce (2002). The red box on the inset map indicates the extent of the respective study areas.

CHAPTER 4

RESULTS AND INTERPRETATIONS

WELL INTERPRETATIONS

Gorgas, USS 29-01-09, Mead Corp. #1, COGC-USX #1, and USS 2-12-01 lie along the path of the cross-section (Fig. 9). Unit 5 is present in all wells; however, the top of the unit lies above the erosional surface in all wells. At Plant Gorgas, Rutter (2012) interpretes 707 m of Unit 5, 173 m of Unit 2, and 349 m of Unit 3. Unit 4 was only partially penetrated, but a thickness of ~1,524 m was established utilizing seismic interpretations, which placed the top of Unit 5 at a depth of ~2,820 m. While the top of Unit 1 was imaged by seismic data at Plant Gorgas, basement was not imaged, and a thickness was not established for Unit 1. Individual formations for USS 29-01-09 were interpreted by Pashin et al. (2011). The USS 29-01-09 well penetrated approximately 1,052 m of Unit 5, 250 m of Unit 4, 370 m of Unit 3, and TDs 332 m into Unit 4. The interpretations from Plant Gorgas and USS 29-01-09 established log responses for the formation tops. These, coupled with drilling reports and sample logs, allowed for interpretation of the remaining wells. Mead Corp. #1 penetrated 669 m of Unit 5, 143 m of Unit 4, and reached TD 195 m into Unit 3. COGC-USX #1 penetrated ~1,323 m of Unit 5, 261 m of Unit 4, and 257 m of Unit 3, reaching TD 274 m into Unit 2. USS 2-12-01 penetrated ~2,174 m of Unit 5, 346 m of Unit 4, 288 m of Unit 3, and 446 m of Unit 2, reaching TD 283 m into Unit 1. The thicknesses used in the cross-section and an explanation of the thicknesses are at the beginning of the discussion section.

SEISMIC INTERPRETATIONS

The interpretation of seismic Line 691-12 (Fig. 16B) consists of a forward-propagating thrust sequence with four main thrust faults that branch off from a basal detachment. While the seismic data cross other large faults, such as the Spring Creek Thrust (SCT) and Elliotsville Thrust (ET), toward the southeastern part of the line, their branch points lie beyond the extent of the seismic data to the SE. Basement along the profile is at a minimum depth of ~4,700 m in the BWB and at a maximum depth of ~7,200 m in the BGS (Fig. 16B). The décollement cuts horizontally through Unit 1 from SE to NW and ends approximately 1.4 km NW of the last basement fault scarp, slightly above basement (Fig. 16B). The décollement may continue to the NW, but it cannot be identified on the seismic data. Moving from SE to NW, the first thrust is the HT, which ramps up from the décollement at approximately 22-23°. Only Unit 1 is interpreted in the HT hanging wall, which is confirmed by the surface geology, while the entire stratigraphy along with the TA and the BES are interpreted in the footwall. Northwest of this location, the seismic line follows a path that is not perpendicular to the thrust belt; thus, the cross-section is governed by the surface geology and the location of the décollement at depth (Fig. 4). The second thrust will be referred to as the Chowns Thrust (CT) and ramps from the décollement at approximately 20-21°, cutting through the entire stratigraphy (Fig. 16B). The CT is not mapped at the surface for two reasons: (1) the fault only juxtaposes Unit 5 against itself and (2) the fault crops out in the residential area of Parkwood, AL. However, the fault is interpreted from the location of reflector terminations (Fig. 16B). The third fault ramps up at an angle of approximately 26° and creates an imbricate fan consisting of Unit 1 against the fourth fault, the JVT.

The BCT separates the relatively undeformed foreland units of the BWB from units in the Alleghanian thrust belt and ramps up at an angle of approximately 15°, cutting through the entire stratigraphy and bringing Unit 1 to the surface. The OVT and BCT are part of an imbricate fan that branches off from the JVT. The OVT branches off of the JVT at an angle of 30° and at a depth of 1,265 m (Fig. 16B). In this location, only Unit 5 is carried in the OVT hanging wall (Fig. 9). The BCT is the frontal fault and branches off of the OVT at an angle of 30° and depth of 1,000 m. Units 5 through 2 are present in the BCT hanging wall. A fault propagation breakthrough fault is interpreted, along with two blind thrusts. The breakthrough fault ramps from the BCT at approximately 20°, while the two blind thrusts ramp at approximately 26° and 30°. These faults result in an anticlinal, fault propagation fold that is cored by a distorted section of Unit 2 and displays steeply-dipping units in the forelimb. A blind thrust is interpreted approximately 2 km from the NW end of the décollement, creating an anticline where the décollement tips out directly below the BCT (Fig. 16B).

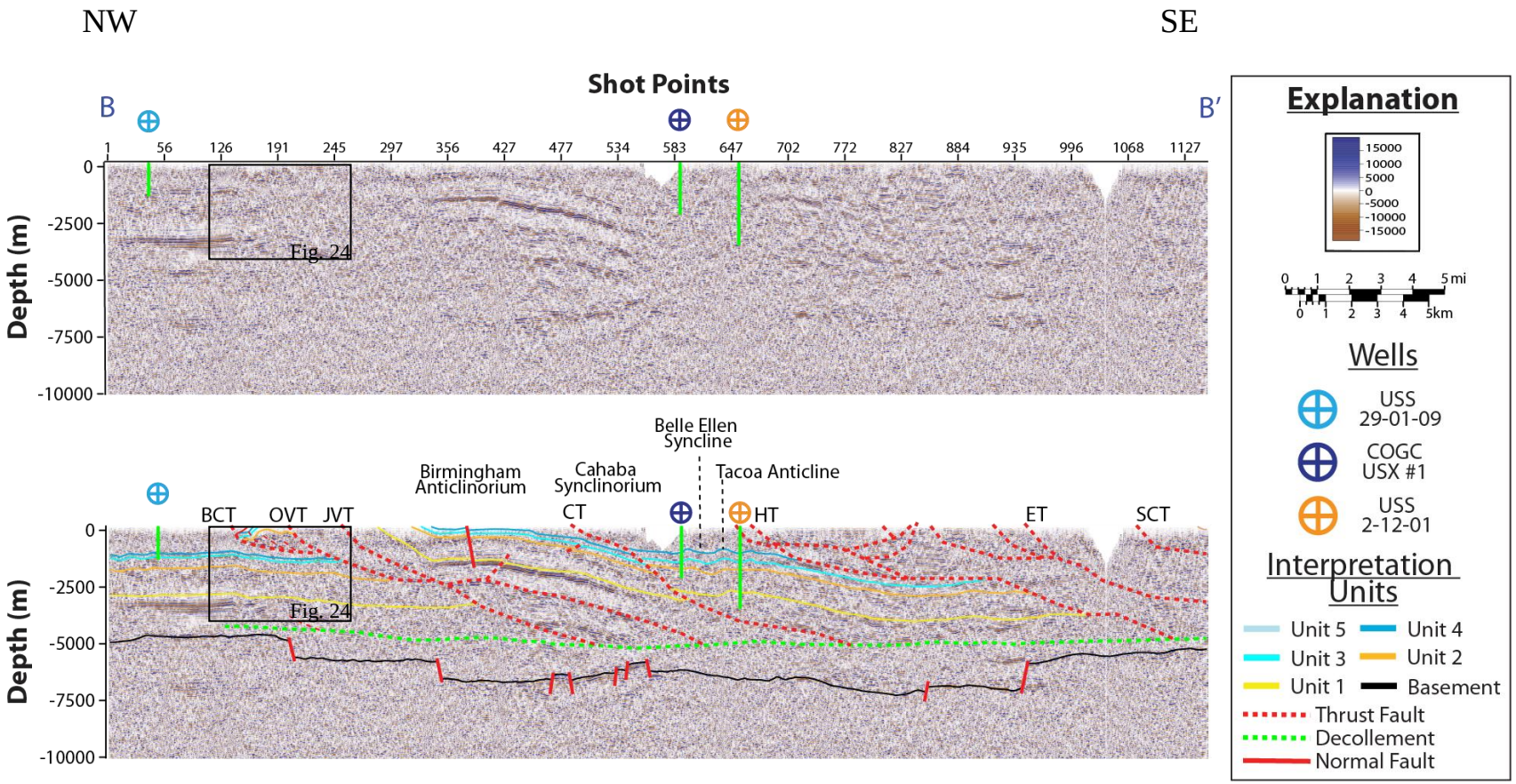

Figure 16. Depth converted seismic data from Line 691-12 (A) without interpretations and (B) with interpretations. BCT=Blue Creek Thrust, OVT=Opossum Valley Thrust, JVT=Jones Valley Thrust, HT=Helena Thrust, ET=Elliotsville Thrust, SCT=Spring Creek Thrust. Vertical Exaggeration = 1x. Refer also to Plate 1.

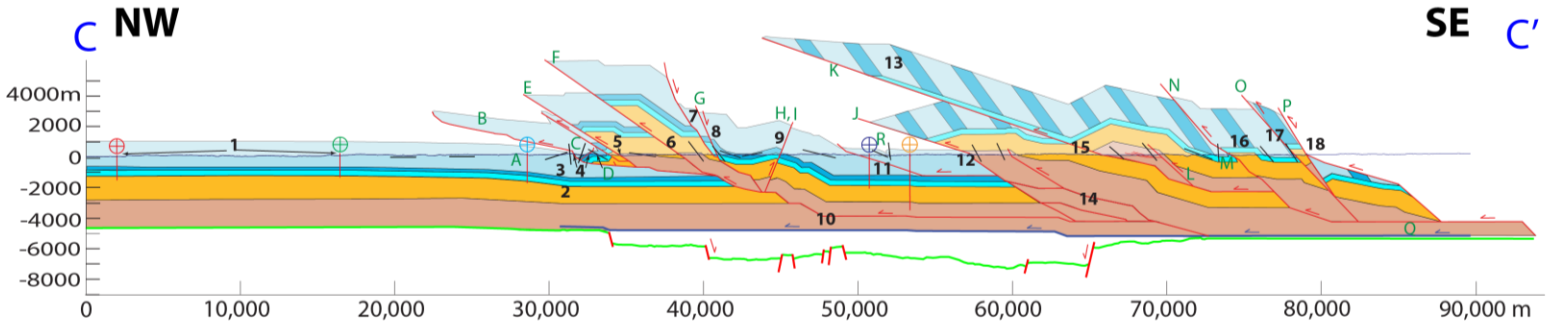

Structures

A Coalburg Syncline
B Blue Creek Thrust (BCT)
C Blue Creek Syncline (BCS)
D McAshan Mtn. Backthrust (MMT)
E Opossum Valley Thrust (OVT)
F Jones Valley Thrust (JVT)
G Potter Normal Fault
H Dickey Springs Anticline
I Dickey Springs Thrust (DST)
J Helena Thrust (HT)
K Elliotsville Thrust (ET)
L Spring Creek Thrust (SCT)
M Roberta Syncline
N Dry Creek Thrust (DCT)
O Shelby Springs Thrust (SST)
P Talladega-Cartersville Thrust (TCT)
Q Basal Detachment
R Tacoa Anticline/Belle Ellen Syncline (TA/BES)

Wells

Gorgas
Mead Corporation #1
USS 29-01-09
COGC-USX #1
USS 2-12-01

Interpretation Units

Unit 5
Unit 4
Unit 3
Unit 2
Unit 1
Unit 5 and 4 Undiff.

Basement
Fault
Decollement
Dip Indicators

Annotations

1) Dip of Units 1-3 in the foreland is approximately 0.5°. Formation tops were taken from Plant Gorgas (Rutter, 2012) and extended to Mead #1.

2) Unit 4 thins toward the southeast as seen on seismic data.

3) Minimum thickness for Unit 1 was taken from this location.

4) At the surface, th dip of BCT is approximately 68° and MMT is approximately 35° determined from 1:24000 geologic map (Irvin and Gates, 2008)

5) Dip of OVT at the surface is approximately 31° from seismic data.

6) Dip of JVT at the surface is approximately 35° from seismic data.

7) This normal fault cuts units 1 through 4, juxtaposing units 3 and 4. It intersects the surface at approximately 52°. The OVT and JVT thrust sheets both carry half thickness of Unit 5.

8) Dip of the Potter Fault at the surface is approximately 65° determined from 1:24000 geologic map (Ward and Osborne, 2005). It joins the normal fault from 7 at approximately 100 m below the erosional surface.

9) Dip of DST at the surface is approximately 68° determined from 1:24000 geologic map (Ward and Osborne, 2005). It carries the Dickey Springs Anticline in its hanging wall.

11) Interformational fault within Unit 5. Carries the Tacoa Anticline and Belle Ellen Syncline in the hanging wall.

12) Dip of HT at the surface is approximately 50° at the surface determined from 1:24000 geologic map (Osborne and Ward, 1996). This thrust sheet carries the full thickness of Unit 5.

13)This long ramp is inferred from a need to fill space between the ET and the HT.

14) This imbricate fan structure makes room for the full length of the Unit 5 half thickness in the JVT and OVT hanging walls to be restored on top of the half thickness in the JVT footwall.

15) Dip of ET at the surface is approximately 18° at the surface determined from 1:24000 geologic map (Osborne, Ward, and Irvin, 1998).

16) Dip of DCT at the surface is approximately 32°, taken from Brewer (2004). The Roberta Overturned Syncline developed in the DCT footwall.

17) Dip of SST at the surface is approximately 48°, taken from Brewer (2004).

18) Dip of TCT at the surface is approximately 25°, taken from Brewer (2004). The normal fault developed at approximately 57° and connects the TCT and SST at approximately 2400 m below the erosional surface.

Figure 17. Completed, unrestored cross-section, including descriptions of the cross-section features.

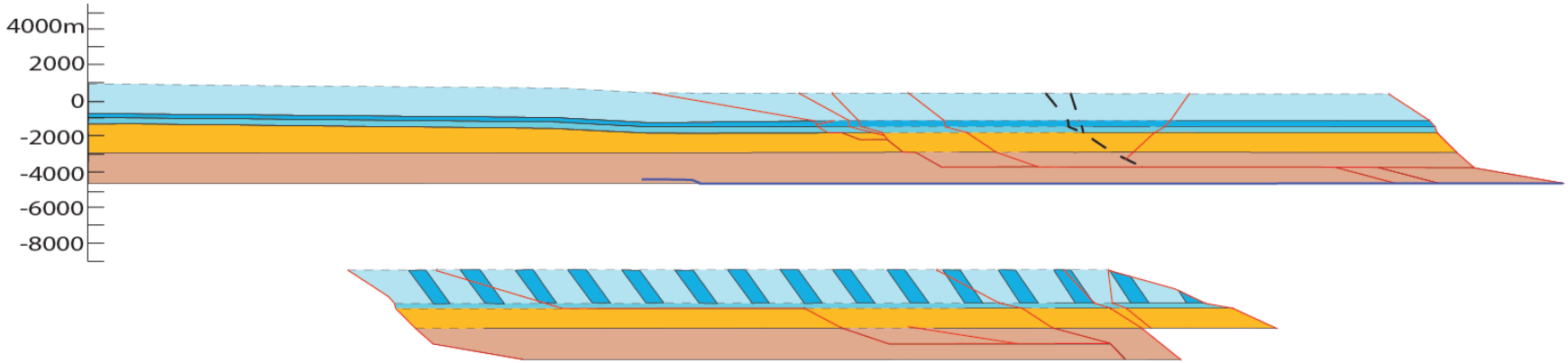

Figure 18. Completed, restored cross-section

CHAPTER 5

DISCUSSION

BALANCED CROSS-SECTION

The unit thicknesses used for structural interpretation are from well log and seismic interpretations (Fig. 17). Transparent units above the surface of the Earth represent units that were once above the erosional surface but have been eroded to account for missing length; however, no attempt is made to determine when the erosion occurred. Minimum lengths are used to minimize shortening. Because the top of Unit 5 is always above the erosional surface, a minimum thickness of 1,571 m is used because the top of Unit 5 is placed ~520 m above the erosional surface at well USS 29-01-09. This thickness falls within the 0-3,505 m range established by Raymond et al. (1988) for the Pottsville and Parkwood formations and places the top of Unit 5 above the erosional surface in all the wells. Unit 4 thickens from 169 m at Plant Gorgas to approximately 350 m at the frontal thrust cutoff. This thickness is maintained to the SE through the rest of the cross-section as the thicknesses are similar in wells COGC-USX #1 and USS 2-12-01. The thickening of Unit 4 to the SE can be explained by the gradation change from the shallow water carbonate rock, the Bangor Limestone, in the NW into the deeper marine Floyd Shale in the SE (Thomas, 1972, 1995). Unit 3 maintains a relatively constant thickness of ~350 m as the Tuscumbia Limestone is a regionally persistent formation. Unit 2 thins to the SE, from 1,448 m at Plant Gorgas to 1,054 m at the frontal thrust cutoff. A possible explanation for the thickness change could be that subsidence rates in the Knox Group carbonate rock varied

along the gently sloping, muddy carbonate ramp or that there was water depth variability in the shelf elevation (Raymond et al., 1988; Montanez and Read, 1992). A thickness for Unit 1 was not initially established at the Gorgas well because the well did not penetrate Unit 1 or basement, and only the top of Unit 1 was imaged on seismic data (Rutter, 2012). However, a thickness of 1,850 m is determined for Unit 1 at well USS 29-01-09 because the seismic data near that well show both the top of the unit and basement (Fig. 16B). This thickness was projected to the NW to Mead Corp. #1 and then to Plant Gorgas, which lies approximately 15 mi (24 km) NW of the northwest most extent of the seismic re-projection (Fig. 9), and a pin line was established in the foreland.

A thickness issue was encountered between the TCT and Shelby Springs Thrust (SST; N, O, Fig. 17). Unit 2 is present at the surface between the two thrusts. This implies that all of the units were emplaced and Units 3-5 and part of Unit 2 were eroded, leaving the rest of Unit 2 and Unit 1 in the subsurface. However, there is not enough room between the two thrusts to fit all of the units. The SST originally emplaced Units 1-5 above a long flat (Q, Fig. 17), with the TCT on top of the package. A normal fault developed that connected the SST and TCT below the present erosional surface, causing most of the units that were originally emplaced by the SST to be down-thrown and the remaining units to remain above the erosional surface (Fig. 19).

A length problem was also encountered in the hanging wall of the ET (K, Fig. 17). The ET splays off of the DCT, carrying the full thicknesses of Units 5-2, but only a half-thickness of Unit 1. A long flat of half-thickness Unit 1 is needed to restore the ET down. When it is restored, there is missing length in Units 3-5. The ET is extended, along with Units 3-5, to accommodate the missing length.

In addition, a geometry problem was encountered near the Potter Fault. The Potter Fault (8, Fig. 17) is a normal fault with a dip of approximately 65° that juxtaposes parts of Unit 3. On geologic maps (Fig. 9), the relationship between Unit 3 and Unit 2 in the Potter Fault footwall is conformable. However, a normal fault was inferred between Units 3 and 2 to accommodate the full thickness of Units 2-5 in the Potter Fault hanging wall. The conformable nature of Units 3 and 2 would have made this fault (7, Fig. 17) difficult to recognize in the field. This normal fault initiated first, cutting Unit 2 at approximately 60°. The Potter Fault then initiated simultaneously with the Dickey Springs Thrust (DST), causing the block to rotate.

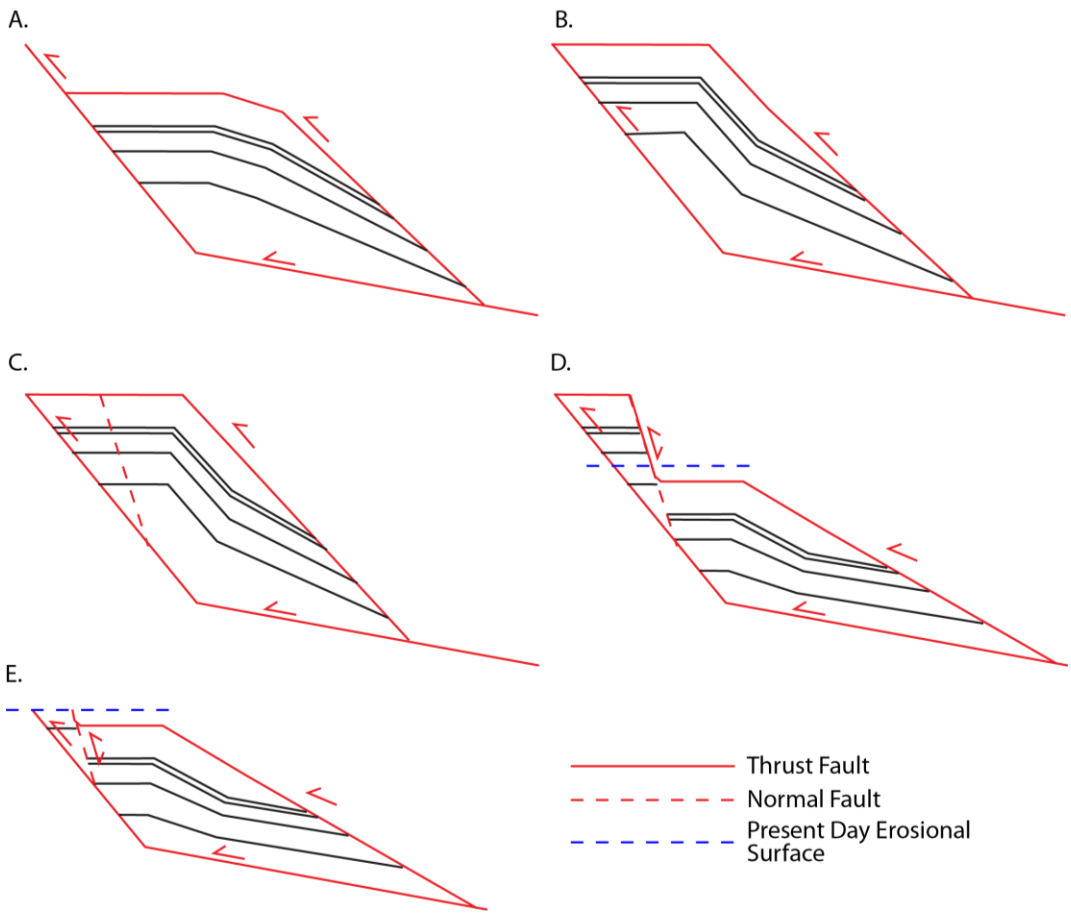

Figure 19. Simplified cartoon of the kinematics of the Talladega-Cartersville Thrust (TCT) emplacement. The figure is not to scale and is not balanced.

When the Potter Fault block is restored, a half-thickness of Unit 1 must also be restored. This half thickness is incorporated in the JVT and OVT hanging walls (6, Fig. 17). To account for this, a long flat section is inferred (10, Fig. 17). This flat extends SE and merges into the décollement at approximately 15°, directly beneath the ET.

In the restoration of the cross-section (Fig. 18), all faults dip toward the east as they should, and the cross-section is restorable and viable. Unit 1, the oldest unit, continues to the south underneath the TSB. This is not shown in the restoration because the cross-section terminates at the TSB at the surface; thus, the balance for Unit 1 is not correct because more of the unit exists to the southeast. Balancing of the cross-section yields a minimum shortening estimate for the Alleghanian thrust belt in central Alabama using the equation in the Methods section. This cross-section has a minimum of 30 km (24 %) shortening. An error of +/- 10% should be assumed for this estimate as the cross-section path is approximately 10°-15° from the direction of tectonic transport. Offsets of as much as 20° are considered acceptable (Price, 1981, Woodward et al., 1989).

KINEMATIC DEVELOPMENT OF THE BALANCED CROSS-SECTION

In a fold-thrust belt, thrust faults can be separated into in-sequence and out-of-sequence faults. In-sequence thrust faults become younger towards the foreland (McClay, 1992). Out-of-sequence thrust faults do not follow the same progression. If a younger fault is closer to the hinterland than an older fault, it is considered out-of-sequence.

As a cross-section is being restored, each fault-block is being moved to its pre-deformed state (Figs. 17, 18, and 19). Through this process, the order in which faults were formed can be determined. Thus, although the restoration is completed from youngest to oldest, the kinematic evolution is described oldest to youngest. The TCT (P, Fig. 17) is the oldest fault in the

sequence, placing Neoproterozoic to Cambrian metamorphic rocks of the Talladega Slate Belt over flat-lying passive margin sedimentary rock. The TCT is followed by emplacement of the ET (K, Fig. 17). Note that the ET has only half of the total thickness of Unit 1. There are three out-of-sequence faults between the TCT and ET, making the timing of slip difficult to determine in the thrust belt. The first of these out-of-sequence faults is the SST (O, Fig. 17), which branches off of the initial flat of the ET at 46°. The second is the DCT (N, Fig. 17), which branches off of the ET where it transitions from its second ramp to its second flat. The third is the SCT (L, Fig. 17) that branches off of the ET at 43° and that helped to form a hanging wall anticline above the erosional surface. There are also some small faults that branch from the SCT, but are too small to significantly offset stratigraphy.

Because the ET carries only half of the total thickness of Unit 1, the remaining half of the thickness needs to be somewhere in the thrust belt. In Figure 17, the Unit 1 thrust sheets (marked with "14") are the remaining Unit 1 stratigraphy. To move these thrust sheets into that location, the thrust sheets must have first been emplaced and pushed toward the foreland, over the top of the HT before the HT was emplaced (J, Fig. 17). Then, the HT must have been emplaced and over-thrust these two unit 1 thrust sheets. In the hanging wall of the HT, there is an out-of-sequence fault, the timing of which is unknown (Fig. 17). In the footwall of the HT, there is also an out-of-sequence thrust within Unit 1 and carried by the JVT thrust sheet. The timing of this fault is after the HT formed but how long after is unknown.

After emplacement of the HT, the next large thrust sheet that is emplaced is the JVT (F, Fig. 17). Two out-of-sequence faults merge with the JVT in the hanging wall: the Potter fault and DST (G and I, Fig. 17). The Potter fault is a single normal fault at depth but branches near the surface to produce two normal faults (7 and 8, Fig. 17). The DST is a backthrust and forms the

Dickey Springs Anticline (DCA) as a hanging wall anticline. The timing of the Potter fault and DST is unknown. Simultaneous movement on the Potter fault and DST resulted in rotation of a portion of the JVT hanging wall. After emplacement of the JVT, the OVT was emplaced (E, Fig. 17). Between the OVT and the BCS, there is another small thrust emplaced after the OVT. After emplacement of the small thrust, the frontal thrust of the thrust belt was emplaced. This is the BCT (B, Fig. 17), the youngest in-sequence fault interpreted on the cross-section. In the hanging wall of the BCT, one out-of-sequence fault, the McAshan Mountain Backthrust (MMT; D, Fig. 17) exists, also with unknown timing.

COMPARISON WITH OTHER INTERPRETATIONS

Maher (2002), Pearce (2002), Gates (2006)/Robinson et al. (2008), and Bailey (2007)/Robinson et al. (2012), utilized seismic lines from the same VASTAR survey (Fig. 2). Minimum shortening estimates from these studies are summarized in Table 3. Maher (2002) estimated 3,720 m of minimum shortening in the Knox-Pottsville interval, or approximately 5%, and 4,520 m of shortening in the Rome-Conasauga interval, equal to approximately 6% shortening across the Wills Valley Anticline (2, Fig. 2). Gates (2006) and Robinson et al. (2008) calculated 5.4% minimum shortening for a nearly 24 km long profile across the Wills Valley Anticline (1, Fig. 2), similar to the shortening estimate of Maher (2002). Pearce (2002) estimated 34 km of minimum shortening, or approximately 29%, across an 85 km long profile through the Alabama Valley and Ridge (3, Fig. 2). Cross-section 16 from Thomas and Bayona (2005) is located in the current study area and yields a minimum shortening estimate of ~33% (Fig. 22). Bailey (2007) and Robinson et al. (2012) balance the same cross-section and estimate a minimum shortening of 26% for interpretation 2 and 33% for interpretation 1 (5, Fig. 2). Additionally, cross-section B from Brewer (2004; Fig. 22) yields approximately 55 km (38%) of

shortening. The minimum shortening estimates from this study are most similar to those calculated by Pearce (2002), Bailey (2007)/Robinson et al. (2012), Thomas and Bayona (2005), and Brewer (2004), which are discussed further below.

Interpretations from Pearce (2002)

Pearce (2002; Fig. 2) construct a balanced cross-section with a single basal décollement above the BGS (1, Fig. 20) that propagated from southeast to northwest. The décollement dips slightly into the graben system as it comes off the most southeastern graben, cutting down stratigraphy in the footwall, and it gently ramps back up as it continues onto the platform to the northwest. The cross-section also incorporated 11 thrust faults, including 2 large, foreland-dipping backthrusts and one hinterland-dipping thrust. The TCT and HT (2 and 3, Fig. 20) are the only faults Pearce (2002) and the current study have in common. In both cross-sections, the HT has a long, sweeping profile with at least one out-of-sequence fault branching off at a high angle. Additionally, the current study interprets multiple thrust sheets in the Conasauga Formation in the HT footwall. Pearce (2002) interprets an imbricate fan located ~12.5 km to the northwest of the branch point of the HT, in the footwall of the Argo fault (4, Fig. 20). The branch point of the TCT is not present on the interpretation of Pearce (2002); however, it likely branches southeast of the section where there is no interpretation. Pearce (2002) interprets a long fault, the Pell City fault (PCT) that branches off of the TCT and places a large block of Knox Group above the regular stratigraphy. The forelandward structures of Pearce (2002) are not similar to those in the current study.

Interpretations from Bailey (2007) and Robinson et al. (2012)

Bailey (2007) and Robinson et al. (2012; Fig. 2) interpret a section of the fold-thrust belt

that lies beneath Coastal Plain sediments, rendering direct observation impossible. Because of this data limitation, two interpretations were made (Fig. 21). Both interpretations incorporate a simple structural geometry, with two detachments (one upper, one lower) and three thrust faults. Two of these faults incorporate a ramp-flat geometry that is common for faults in the present study, while the third ramps up directly to the surface at the northern boundary of the graben system. In their first interpretation (interpretation 1), all three faults are brought to what was the

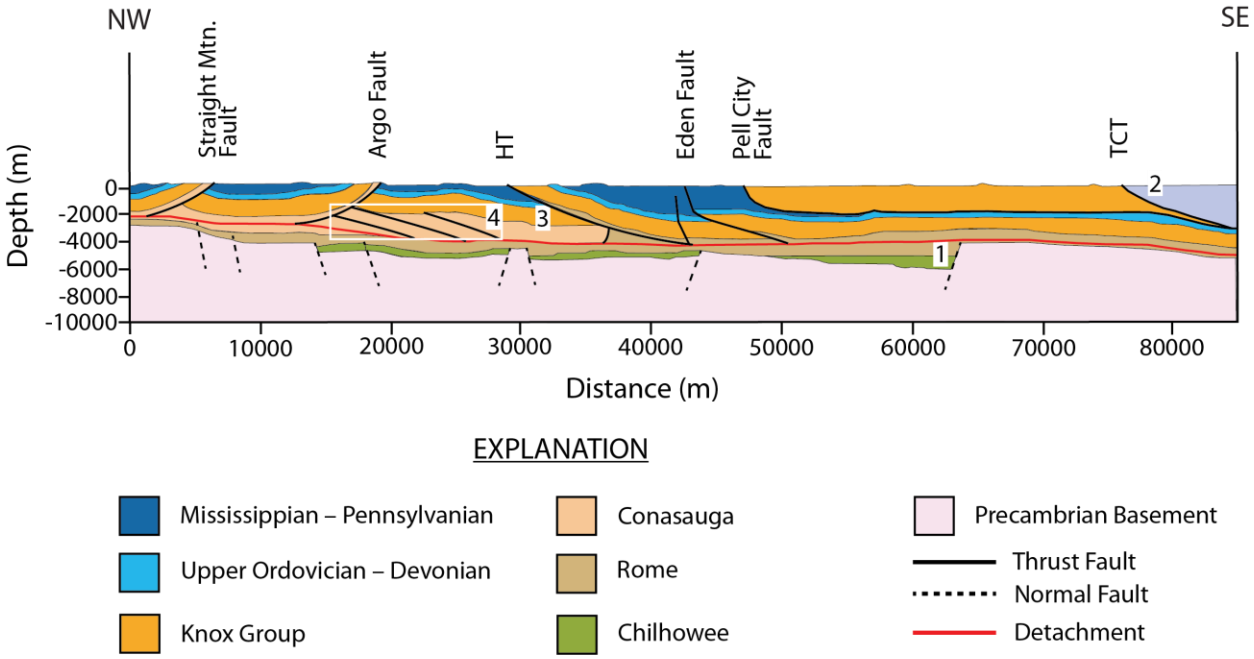

Figure 20. Cross-section, modified from Pearce (2002), pre-restoration.

topographic surface at that time, while their second interpretation (interpretation 2) interprets the most hinterlandward thrust as a blind thrust (1, Fig. 21 B). Thus, toward the south, the thrust belt has a more simple geometric architecture when compared to central Alabama. In addition, the basal décollement from Bailey (2007) and Robinson et al. (2012) does not extend into the BWB (2, Figs. 21A and 21B) as it does with Pearce (2002), Thomas and Bayona (2005), and this study.

Both interpretations incorporate horst and graben structures that are inferred to be the southern expression of the BGS, with a single graben in interpretation 1 (3, Fig. 21A) and a graben, half-graben, and horst in interpretation 2 (3, Fig. 21B). The size of the grabens is smaller than similar structures in other studies, indicating that the BGS dies out to the southwest. The deepest graben from Bailey (2007) is approximately 650 m deep. This contrasts to the 2,000 m estimate by Pearce (2002) and 1,300 m interpreted in this study, both of which incorporate multiple graben structures.

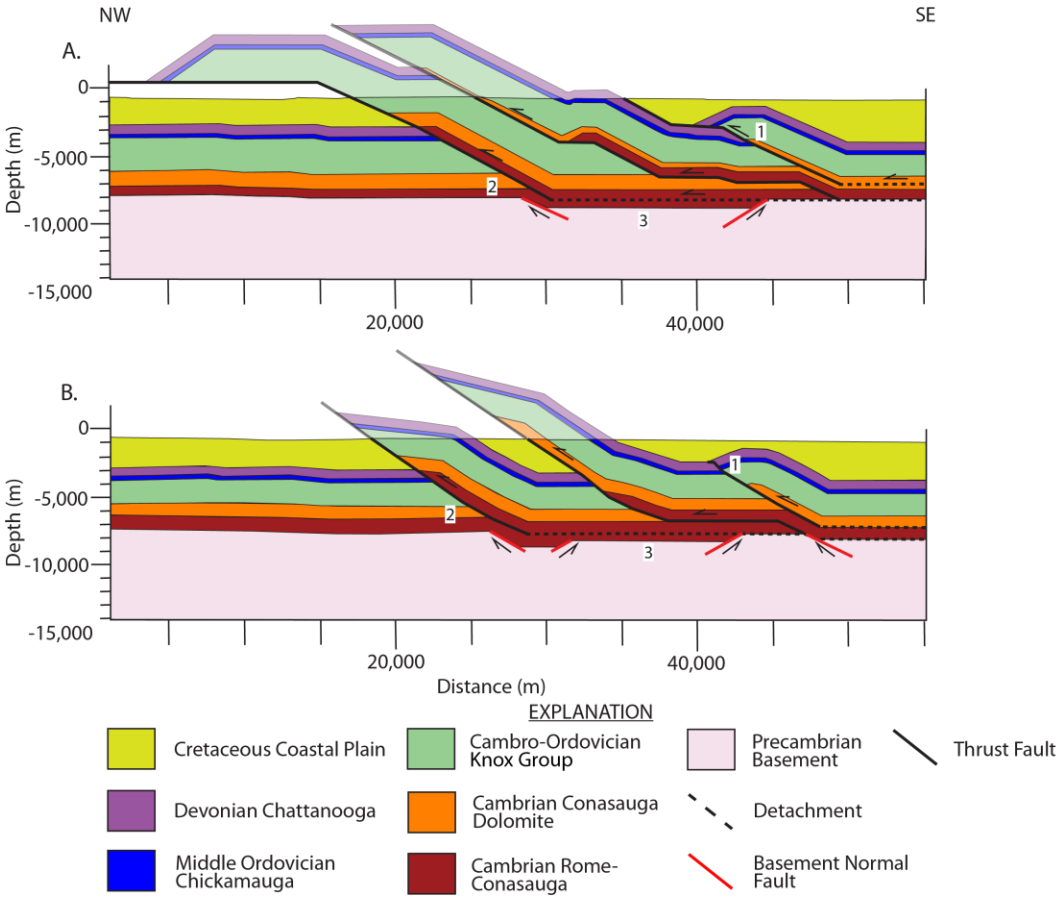

Figure 21. Balanced cross-sections. (A) Interpretation 1 and (B) Interpretation 2 modified from Bailey (2007) and Robinson et al. (2012).

Interpretation from Thomas and Bayona (2005)

Thomas and Bayona (2005) constructed 18 cross-sections along the fold-thrust belt in Alabama. Although the work is based on seismic data, these data are not provided. Their cross-section 16 is within the study area (Fig. 22). Like the cross-section from the current study, cross-section 16 employs a total of 15 thrust faults (Fig. 23). Similar to Pearce (2002), Thomas and Bayona (2005) interpret a single décollement that propagates from southeast to northwest above the BGS, starting level with the basement in the southeast. However, to the northwest, the décollement cuts up through the Rome-Conasauga interval in the footwall (1, Fig. 23) when it reaches the first basement horst. The décollement then follows basement topography, cutting down-section in the footwall to the northwest of the basement horst (2, Fig. 23) and then cutting up-section in the footwall again as it reaches the northwestern boundary of the graben system (3, Fig. 23). In the present study, the décollement is at the top of the basement; however, the southeastern boundary of the graben system is interpreted as a platform. The difference in geometry results in the décollement being above the basement structures, allowing it to continue unobstructed to the northwest. Furthermore, the décollement of Thomas and Bayona (2005) cuts down-section in the stratigraphy of the footwall and is in violation of the rules of balancing cross-sections (Woodward, 1989). In the present study, the décollement does not propagate down-section in the initial graben, instead ramping up slightly before propagating horizontally to the northwest (Fig. 17).

In Thomas and Bayona (2005), six large thrust faults ramp up from the décollement at 6-25° (Fig. 23). The geometry of the TCT (4, Fig. 23) is similar to that interpreted in the current study, with the thrust ramping up from the detachment and shallowing toward the surface, placing TSB metamorphic rocks over top of Alleghanian thrust belt rocks. The next fault to the

northwest (5, Fig. 23) ramps up to a long flat approximately 7,800 m long, repeating the underlying stratigraphy before connecting to the YT, creating an imbricate fan. The YT ramps from the décollement at approximately 10° and maintains a dip of 18-38° along an 11.5 km profile until it crops out at the surface, where Thomas and Bayona (2005) interpret Knox Group

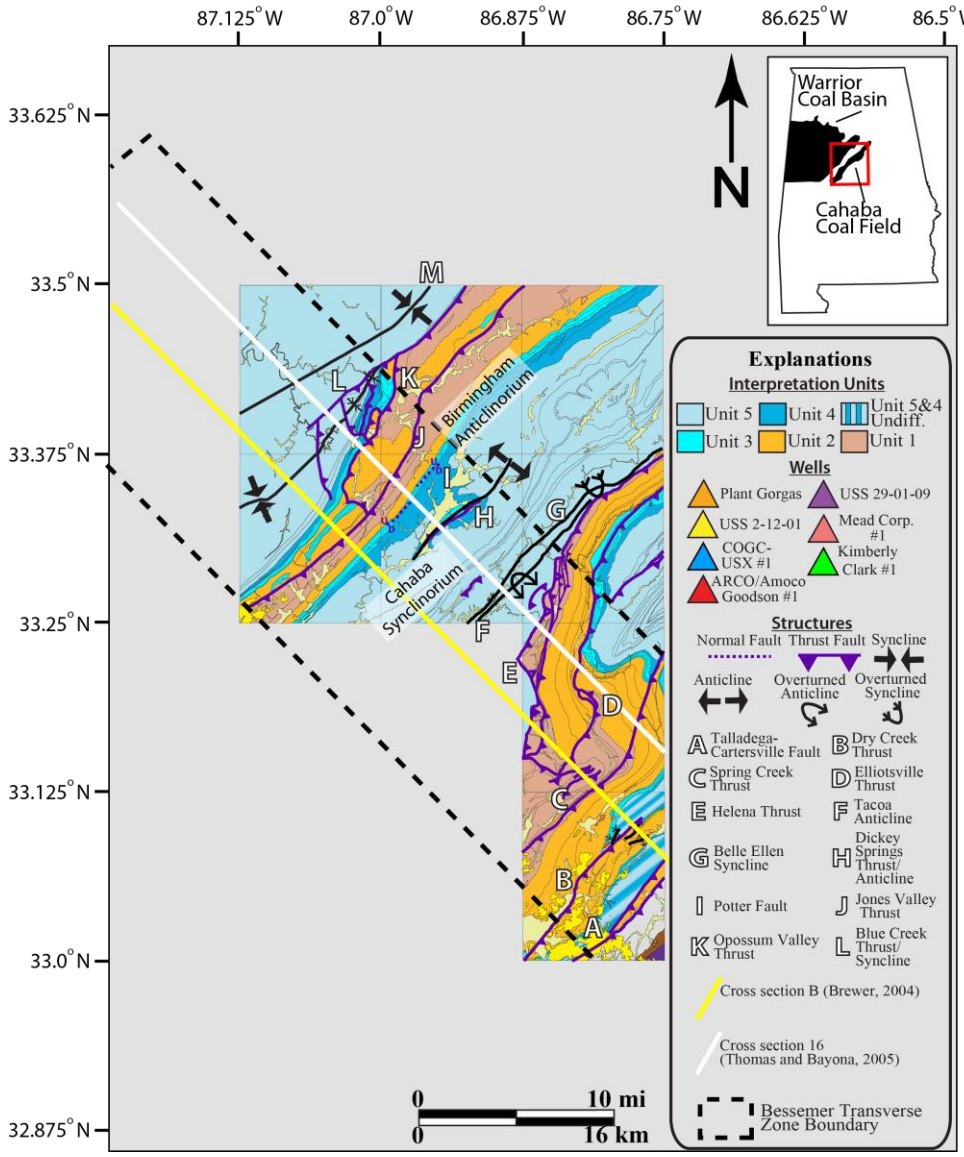

Figure 22. Geologic maps from Figure 9. The yellow line marks the location of cross-section B from Brewer (2004). The white line marks the location of cross-section 16 from Thomas and Bayona (2005).

carbonate rock in the hanging wall and Pottsville Formation clastic rock in the footwall. The surface expression of the YT ends approximately 11.3 km (7.0 mi) to the northeast, but it is not interpreted in the subsurface on the section from the current study.

In Thomas and Bayona (2005), the HT ramps from the décollement at 7°, compared to 30° in the current study. Thomas and Bayona (2005) interpret a ramp-flat-ramp geometry on the HT (6, Fig. 23) that brings Conasauga Formation to the surface in the hanging wall, which is also interpreted in this study. In Thomas and Bayona (2005), an out-of-sequence thrust branches from the HT, which in turn produces two additional thrusts (7, Fig. 23). These three faults form an imbricate fan and contribute to the formation of the COO. In the present study, the HT ramps directly up to the surface but has two Unit 5 thrust sheets in its footwall (14, Fig. 17). Interpretations from Szabo et al. (1988) and Brewer (2004) indicate that the COO dies out to the northeast of the section examined in this study.

The next fault to the northwest of the HT, the OVT, ramps up from the décollement at 15° and frames the southeastern edge of the Bessemer Mushwad, following an 18.5-km-long ramp-flat profile to the surface (8, Fig. 23; Thomas and Bayona, 2005). Two major faults branch off from this fault. The first is the JVT, which branches off at approximately 35° and thrusts Conasauga Formation above a thin section of Knox Group, consistent with the interpretation of the JVT from this study (Fig. 17). A backthrust branches off the JVT, creating a rotated block in the JVT hanging wall (9, Fig. 23), that is also consistent with the interpretation of the DST (Fig. 17) from this study. However, Thomas and Bayona (2005) do not interpret any normal faults at this location. The current study interprets two normal faults: the Potter fault, which is interpreted on maps, and another normal fault (normal fault 2) that merges with the Potter fault in the subsurface. The OVT from Thomas and Bayona (2005) ramps to the surface at 28° bringing the

Conasauga Formation and Knox Group to the surface in the hanging wall, consistent with interpretations from the current study. A splay fault branches off of the OVT, exposing Knox Group at the surface, also consistent with this study.

A major difference between the interpretation from Thomas and Bayona (2005) and the present study is the presence of the Bessemer Mushwad, a ductile duplex consisting of a thick package of Conasauga shale. Thomas and Bayona (2005) and Brewer (2004) interpret the Bessemer Mushwad in the footwall of the JVT and OVT, above the northwestern boundary of the BGS (Fig. 23). However, neither Pearce (2002) nor the present study interpret a mushwad against the frontal thrust. Thomas and Bayona (2005) and Brewer (2004) interpret the Bessemer Mushwad on seismic data as a zone of incoherent reflectors in the hanging wall of the frontal thrust, the BCT (Fig. 22). Additionally, the Marchant Well (approximately 22.8 mi to the southwest of USS 2-12-01) contains a section of structurally thickened shale of the Conasauga Formation, which are interpreted as the Bessemer Mushwad. The seismic data from the present study shows more coherent reflectors above the most northwestern edge of the BGS (Figs. 16). This allows for interpretations of Units 4-1 to be carried from the foreland to the BCT. Rocks of the Conasauga Formation are interpreted in the hanging walls of the OVT and JVT, but no ductile duplexing is interpreted. A zone of reflectors does exist beneath the JVT and OVT, approximately from shot point 245 to 356, which could potentially be interpreted as incoherent (Fig. 24). However, this zone is more toward the southeast than interpretations from Thomas and Bayona (2005).

Thomas and Bayona (2005) interpret the frontal fault of the fold-thrust belt as the BCT, which dips at 26° as the detachment rises over the northwest limit of the BGS and onto the platform (10, Fig. 22). In the present study, the BCT is also interpreted as the frontal thrust (B,

Fig. 17). However, the BCT does not ramp from the décollement but branches off from the OVT (E, Fig. 17). Thomas and Bayona (2005) interpret two unnamed backthrusts branching off of the BCT (11, Fig. 22). The steeper of the two dips at nearly 70° and connects to the OVT splay fault, while the second is vertical to overturned at the surface. Thomas and Bayona (2005) interpret the end of the décollement approximately 18.4 km northwest of the edge of the BGS (12, Fig. 22). The present study interprets the décollement extending approximately 3 km northwest of the BGS (Fig. 17).

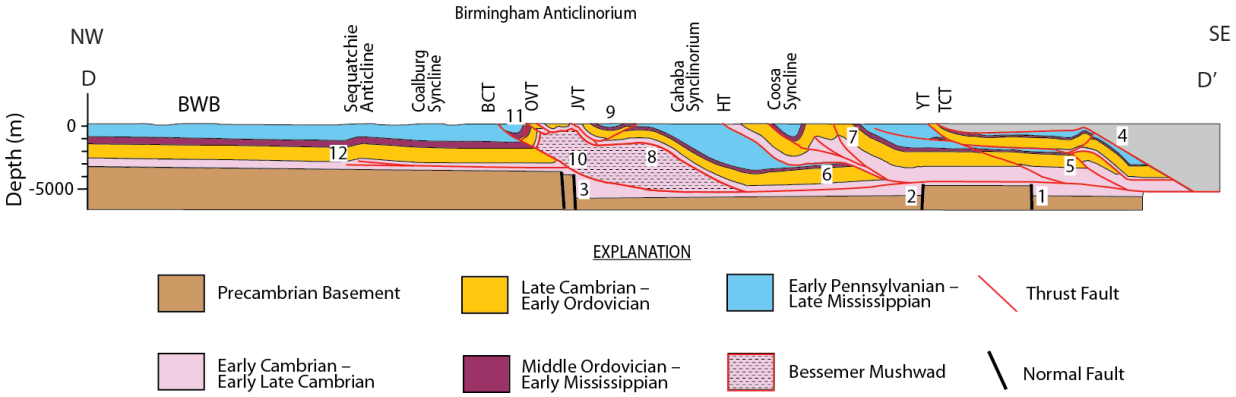

Figure 23. Cross-section 16, modified from Thomas and Bayona (2005), pre-restoration.

Interpretations from Brewer (2004)

Brewer (2004) constructed 12 cross-sections within the Bessemer Transverse Zone (BTZ), 8 trending northwest-southeast and 4 northeast-southwest. Cross-section B from that study (Fig. 22) is the closest to the balanced cross-section in the current study. As with Thomas and Bayona (2005) and the present study, Brewer (2004) incorporates a complex structural geometry. A single décollement underlies 17 total thrust faults. These faults form 5 major thrust sheets: the Talladega, Dry Creek, Helena, Jones Valley, and Blue Creek (Fig. 25). All of these thrust sheets are interpreted on the cross-section from the present study (Fig. 17).

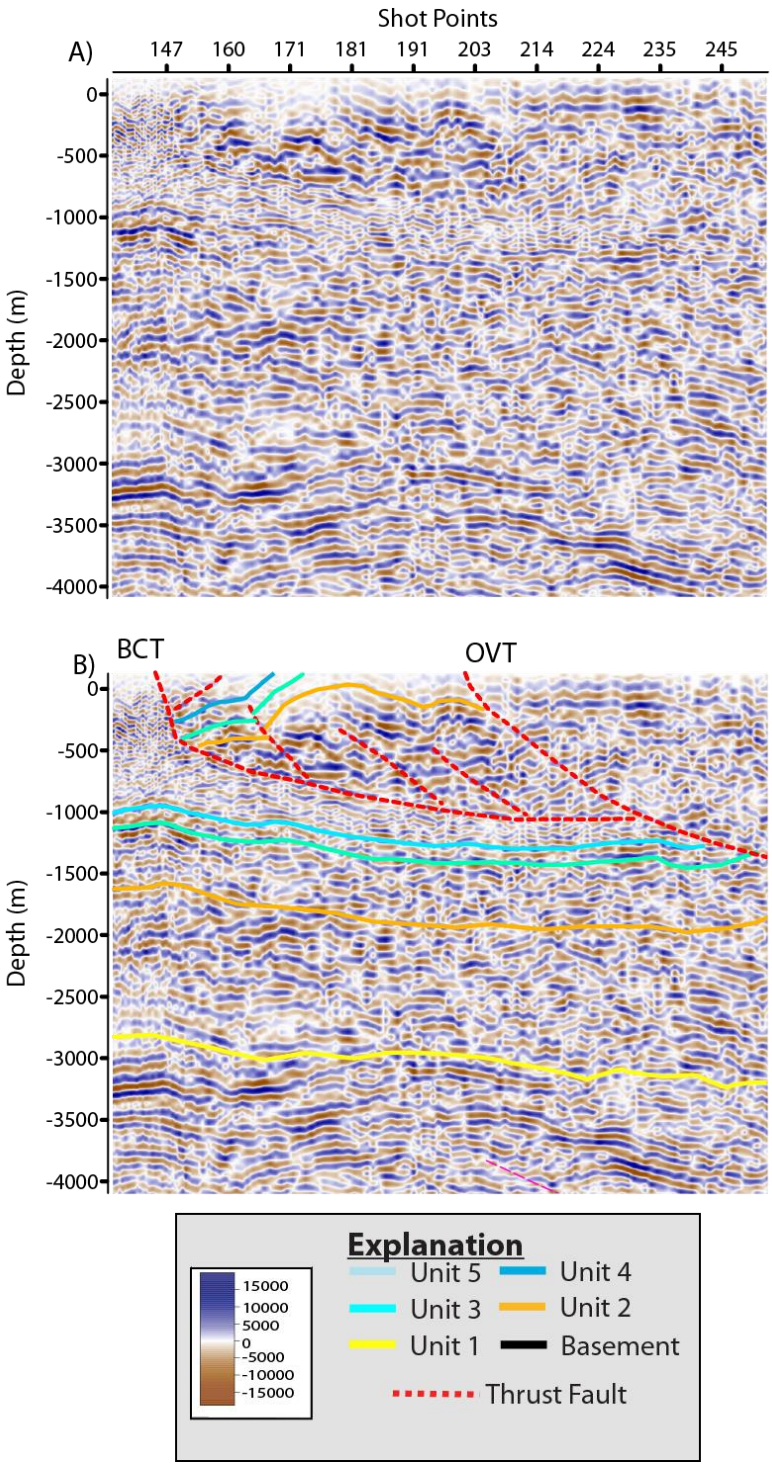

Figure 24. Section of Line 691-12 indicated in Figure 16. This portion highlights the potential absence of the Bessemer Mushwad. (A) Uninterpreted seismic section and (B) interpreted seismic section. BCT = Blue Creek Thrust, OVT = Opossum Valley Thrust.

The décollement propagates from southeast to northwest above the BGS. As in Thomas and Bayona (2005), Brewer (2004) interpretes the décollement beginning level with basement, but ramping up through the Rome-Conasauga interval and over the first horst it encounters (1, Fig. 25). The décollement then cuts down-section through the Rome-Conasauga formation as it comes down off of the horst (2, Fig. 25), continuing to the northwest until it reaches the edge of the BGS, cutting up-section onto the platform (3, Fig. 25). This creates the same problem as in Thomas and Bayona (2005), where the rules of balancing state that a thrust cannot cut down stratigraphy section in the direction of thrusting (Woodward, 1989). In the present study, the décollement remains at a relatively constant depth along the entire cross-section, with a few ramps cutting up section in the direction of propagation.

In Brewer (2004), six large thrust faults ramp up from the décollement. Starting in the southeast, the first major fault is the TCT (4, Fig. 25). The geometry from Brewer (2004) is similar to that found in Thomas and Bayona (2005) and in this study, where it maintains a ramp-flat geometry. However, the interpretation from Brewer (2004) differs because the flat that occurs after the initial ramp up from the décollement is shorter than Thomas and Bayona (2005), approximately 5.5 km compared to 8.6 km, respectively. While the flat interpreted in the TCT from the current study is shorter (5 km), the flat from Brewer (2004) is interpreted deeper than either the current work or Thomas and Bayona (2005) indicate, allowing for a longer ramp from the flat to the surface (4, Fig. 25).

To the northwest, an unnamed fault ramps from the décollement at 44° (5, Fig. 25) and connects to the TCT. The next fault is the DCT, which ramps from the décollement at 36° and continues to the surface with no flat, consistent with the interpretation from the current study. Additionally, an out-of-sequence thrust ramps from the DCT at 71°, transporting Knox Group

rocks to the surface in the hanging wall. Because there is not enough space between the out-of-sequence fault and the TCT, the lengths of required units must remain in space above the erosional surface. The relationship between these two faults is similar to the relationship between the SST and TCT from the present study (Discussion, p. 47). However, the current study incorporates a normal fault to bring the TCT to its present position, while no normal fault is indicated by Brewer (2004).

The next fault to the northwest is the HT, which Brewer (2004) interprets as having a single ramp of 16-22°. Six faults branch from the HT forming an imbricate fan at the surface in the hanging wall (Fig. 25). The HT in the present study (J, Fig. 17) is constructed differently, with only one fault in the hanging wall. In addition, the current study interprets multiple thrust sheets related to the HT in the footwall (14, Fig. 17).

Continuing to the northwest, the next fault is the JVT (Fig. 24). The geometry of the JVT itself is similar between Brewer (2004) and the current study in that it does not incorporate any significant flats and ramps directly to the surface at 13-35°. However, Brewer (2004) does not interpret any normal faults or backthrusts related to the JVT (Fig. 23), while the present study incorporates two normal faults and one backthrust to account for rotation of a section of the JVT hanging wall (G, I, Fig. 17).

The last major fault that branches from the décollement is the frontal BCT. The geometry incorporated by Brewer (2004) is very similar to Thomas and Bayona (2005; Fig. 25), where the BCT ramps directly to the surface. Brewer (2004) interprets one more thrust fault (6, Fig. 23) than Thomas and Bayona (2004). Brewer (2004) also interprets the Bessemer Mushwad in the hanging wall of the BCT (Fig. 23), similar to Thomas and Bayona (2005). As previously explained, the Bessemer Mushwad is not interpreted by the current study.

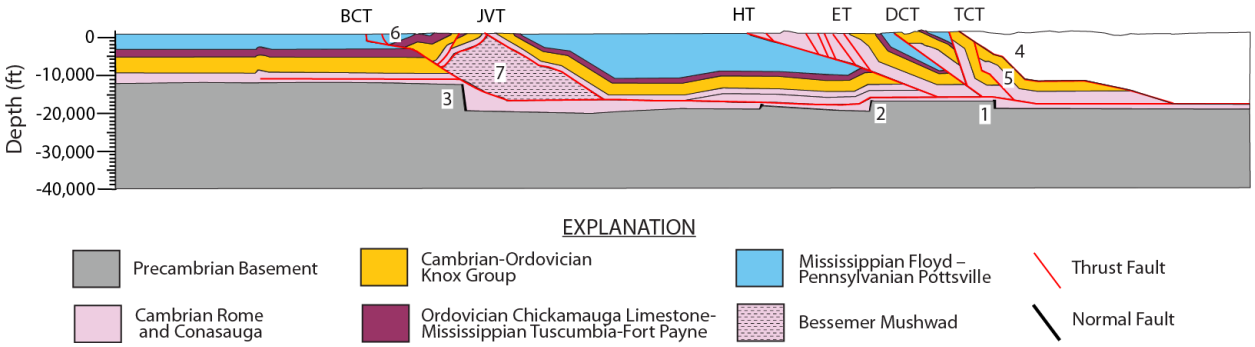

Figure 25. Cross-section B, modified from Brewer (2004), pre-restoration.

Study	ℓ_i	ℓ_f	ℓ_s	% Shortening
This Study	124 km	94 km	30 km	24 %
Bailey (2007) Robinson et al. (2012)	74-78 km	55 km	19 km - 23 km	26% - 33%
Thomas and Bayona (2005)	22.2 cm	14.9 cm	7.3 cm	32.9%
Gates (2006) Robinson et al. (2008)	25.3 km	24 km	1.3 km	5.4 %
Pearce (2002)	119 km	85 km	34 km	29 %
Maher (2002) Pottsville-Knox	73.7 km	70 km	3.7 km	5 %
Maher (2002) Conasauga-Rome	75.7 km	71.2 km	4.5 km	6 %
Brewer (2004)	146 km	91 km	55 km	38%

Table 4. Shortening amounts and percentages from studies conducted along the thrust belt. All of these studies, except Thomas and Bayona (2005) and Brewer (2004), utilized seismic data from the VASTAR survey.

CHAPTER 6

CONCLUSIONS

Seismic data along a profile trending roughly NW-SE in the central Alabama Alleghanian fold-thrust belt was depth converted and interpreted to create an approximately 94 km-long cross-section from the Black Warrior Basin to the Talledega Thrust Belt. The conclusions from this study are as follows:

1) The thrust belt in this part of the Appalachians is a forward propagating thrust belt. The structural geometry interpreted in this study is much more complex than studies conducted in other locations along the thrust belt (*e.g.* Pearce, 2002; Gates, 2006; Robinson et al., 2008; Bailey, 2007; Robinson et al., 2012), commonly displaying out-of-sequence thrusting and backthrusting.
2) Depth to basement is 4,700 m in the Black Warrior Basin and 7,200 m in the Birmingham Graben System, indicating 2,500 m of relief in the horst and graben system.
3) The southeast boundary of the Birmingham Graben System is a platform, disagreeing with interpretations from Brewer (2004) and Thomas and Bayona (2005). This causes the décollement to be interpreted above the Birmingham Graben System rather than within it. The present interpretation prevents the décollement from cutting down stratigraphic section, which allows the cross-section to be viable and balanced.

4) Coherent reflectors exist beneath the frontal thrust fault, indicating that the Bessemer Mushwad may not be present in this location. However, other interpretations exist that interpret the ductile duplex.
5) The minimum shortening estimate from the cross-section balancing is approximately 30 km, or 24%. Because the cross-section line is 10-15° from the tectonic transport direction, an error of +/- 10% should be assumed. This shortening estimate is similar to interpretations from Pearce (2002), Bailey (2007)/ Robinson et al. (2012).

REFERENCES

Asquith, G., and Krygowski, D. (2004) Basic Well Log Analyis, 2nd ed.: AAPG Methods in Exploration Series 16, E.A. Mancini (ed), Tulsa, OK: The American Association of Petroleum Geologists, 244 p.

Bailey, R.M. (2007) Seismic Interpretation and Structural Restoration of a Seismic Profile Through the Southern Appalachian Thrust Belt Under Gulf Coastal Plain Sediments, Master's Thesis, The University of Alabama, Tuscaloosa, AL, 71 p.

Brewer, M.C. (2004) Geometric and Kinematic Evolution of the Bessemer Transverse Zone, Alabama Alleghanian Thrust Belt, PhD Dissertation, University of Kentucky, 235 p.

Butts, C., (1926) The Paleozoic Rocks, *in* Adams, G.I., C. Butts, L.W. Stephenson, and W. Cooke, eds., Geology of Alabama: Geological Survey of Alabama Special Report 14, p. 40-230.

Dahlstrom. C.D.A. (1969) Balanced Cross Sections: Canadian Journal of Earth Sciences, v. 6, p. 743-757.

Drake, Jr., A.A., Sinha, A.K., Laird, J., and Guy, R.E. (1989) The Taconic Orogeny in Hatcher, R.D., Thomas, W.A., and Viele, G.W., eds., The Appalachian-Ouachita Orogen in the United States: Geological Society of America, The Geology of North America, v. F-2, p. 101-176.

Ewing, T.E. (1997) Real Answers for Synthetic Issues, AAPG Explorer 18, #8, p. 24-26.

Gates, M.G. (2006) Structure of Wills Valley Anticline in the Vicinity of Mentone, Alabama, Master's Thesis, University of Alabama, Tuscaloosa, AL, 44 p.

Groshong, Jr., R.H., Hawkins, Jr. W.B, Pashin, J.C.. and Harry, D.L. (2010) Extensional Structures of the Alabama Promontory and Black Warrior Foreland Basin: Styles and Relationship to the Appalachian Fold-Thrust Belt, in Tollo, R.P., Bartholomew, M.J., Hibbard, J.P., and Karabinos, P.M., eds., From Rodinia to Pangea: The Lithotectonic Record of the Appalachian Region: Geological Society of America Memoir 206, p. 579-605.

Hatcher, R.D. (1989) Appalachians Introduction in Hatcher, R.D., Thomas, W.A., and Viele, G.W., eds., The Appalachian-Ouachita Orogen in the United States: Geological Society of America, The Geology of North America, v. F-2, p.1-4.

Hatcher, R.D., Thomas, W.A., Geiser, P.A., Snoke, A.W., Mosher, S., and Wiltscko, D.V. (1989) Alleghanian Orogeny in Hatcher, R.D., Thomas, W.A., and Viele, G.W., eds., The Appalachian-Ouachita Orogen in the United States: Geological Society of America, The Geology of North America, v. F-2, p. 233-318

Hyne, N.J. (1991) Dictionary of Petroleum Exploration, Drilling and Production, Tulsa, OK: Penn Well Corporation, 625 p.

Irvin, G.D.. and Gates, M.G. (2006) Geologic Map of the Concord 7.5-Minute Quadrangle, Jefferson County, Alabama: The Geological Survey of Alabama.

Kearey, P., Brooks, M.. and Hill, I. (2002) An Introduction to Geophysical Exploration 3rd ed., Carlton, Victoria, Australia: Blackwell Publishing Company, 262 p.

Maher, C.A. (2002) Structural Deformation of the Southern Appalachians in the Vicinity of the Wills Valley Anticline, Northeast Alabama, Master's Thesis, The University of Alabama, Tuscaloosa, AL, 45 p.

McClay, K.R. (1992) Glossary of Thrust Tectonics Terms, in *Thrust Tectonics* (ed. McClay, K.R.), Chapman and Hall, London, p. 419-433

Montanez, I.P., and Read, J.F. (1992) Eustatic Control on Early Dolomitization of Cyclic Peritidal Carbonates: Evidence from the Early Ordovician Upper Knox Group, Appalachians: Geological Society of America Bulletin, v. 104, p. 872-886

Neathery, T.L., and Copeland, C.W. (1983) New Information on the Basement and Low Paleozoic Stratigraphy of North Alabama [abs]: Geological Society of America, Southeastern Section, Abstracts with Programs, p. 98.

Osberg. P.H., Tull, J.F., Robinson, P., Hon, R., and Butler, J.R. (1989) The Acadian Orogen in Hatcher, R.D., Thomas, W.A., and Viele, G.W., eds., The Appalachian-Ouachita Orogen in the United States: Geological Society of America, The Geology of North America, v. F-2, p. 179-232.

Osborne, W.E. (1996) Geology of the Helena 7.5-Minute Quadrangle, Jefferson and Shelby Counties, Alabama: Quadrangle Series Map 14, 21 p.

Osborne, W.E., Szabo, M.W., Neathery, T.L., and Copeland, C.W., Jr. (1988) Geologic Map of Alabama (Northeast Sheet): Geological Survey of Alabama, Special Map 220, scale: 1:250,000

Osborne, W.E., Thomas, W.A., Astini, R.A., and Irvin, G.D. (2000) Stratigraphy of the Conasauga Formation and Equivalent Units, Appalachian Thrust Belt in Alabama in Osborne, W.E, Thomas, W.A., and Astini, R.A., eds., The Conasauga Formation and Equivalent Units in the Appalachian Thrust Belt in Alabama: Alabama Geological Society, 37th Annual Field Trip Guidebook, p. 1-17.

Pashin, J.C. (1993) Tectonics, Paleoceanography, and Paleoclimate of the Kaskaskia Sequence in the Black Warrior Basin of Alabama in Pashin, ed., New Perspectives on the Mississippian System of Alabama: Alabama Geological Society, 30th Annual Field Trip Guidebook, pp. 1-28.

Pashin, J.C. (1994) Cycles and Stacking Pattern in Carboniferous Rocks of the Black Warrior Foreland Basin: Gulf Coast Association of Geological Societies Transactions, v. 44, p. 555-563

Pashin, J.C. (2014) *Personal Communication*

Pashin, J.C, Kopaska-Merkel, D.C., Arnold, A.C., and McIntyre, M.R. (2011) Geological Foundation for Production of Natural Gas from Diverse Shale Formations, Geological Survey of Alabama: Open-File Report 1110, 156 p.

Pashin, J. C., Kopaska-Merkel, D. C., Arnold, A. C., McIntyre, M. R., and Thomas, W. A., (2012) Gigantic, gaseous mushwads in Cambrian shale: Conasauga Formation, southern Appalachians, USA, in Bustin, R. M., ed., Shale Gas and Shale Oil Petrology and Petrophysics: International Journal of Coal Geology, v. 103, p. 70-91,

Pashin, J.C., and Rindsberg, A. K. (1993a) Origin of the carbonate-siliciclastic Lewis cycle (Upper Mississippian) in the Black Warrior basin of Alabama: Alabama Geological Survey Bulletin 157, 54 p.

Pashin, J.C., and Rindsberg, A. K., (1993b) Tectonic and paleotopographic control of basal Chesterian sedimentation in the Black Warrior basin: Gulf Coast Association of Geological Societies Transactions, v. 43, p. 391-412.

Patterson, D.J. and Groshong, R.H., Jr. (1989) The Birmingham Anticlinorium: A Large-scale Blind Duplex: Geological Society of America Abstracts with Programs, v. 21, p. A69

Pawlewicz, M.J. and Hatch, J.R. (2007) Ch. 3: Petroleum Assessment of the Chattanooga Shale/Floyd Shale-Paleozoic Total Petroleum System, Black Warrior Basin, Alabama and Mississippi in Geologic Assessment of Undiscovered Oil and Gas Resources of the Black Warrior Basin Province, Alabama and Mississippi: U.S. Geological Survey Digital Data Series DDS-69-1, 23 p.

Pearce, P.J. (2002) Seismic Interpretation and Structural Restoration of a Transect from Murphree's Valley to the Talladega National Forest: The Appalachian Valley and Ridge of Alabama, Master's Thesis, The University of Alabama, Tuscaloosa, AL, 51 p.

Raymond, D.E. (1991) New Subsurface Information on Paleozoic Stratigraphy of the Alabama Fold and Thrust Belt and the Black Warrior Basin, Geological Survey of Alabama: Bulletin 143, 185 p.

Raymond, D.E., Osborne, W.E., Copeland, C.W., and Neathery, T.L (1988) Alabama Stratigraphy, Geological Survey of Alabama: Circular 140, 97 p.

Robinson, D. M., Gates, M.G., and Goodliffe, A.M (2008) Structure of the Wills Valley Anticline, Alabama: Gulf Coast Association of Geological Societies Transactions, v. 59, p. 663-671

Robinson, D.M., Bailey, R.M., and Goodliffe, A.M. (2012) Structure of the Alleghanian Thrust Belt Under the Gulf Coastal Plain of Alabama: Gulf Coast Association of Geological Societies Journal, v. 1, p. 44-54

Rutter, R.S. (2012) A Geophysical Characterization of Stratigraphy in the Eastern Black Warrior Basin Underlying Gorgas Power Generation Plant, Walker County, Alabama, Master's Thesis, The University of Alabama, Tuscaloosa, AL, 82 p.

Szabo, M.W., Osborne, W.E., Copeland, C.W. Jr., and Neathery, T. L. (1988) Geologic Map of Alabama: Alabama Geological Survey Special Map 220, scale 1:250,000.

Robinson, D.M., Bailey, R.M., and Goodliffe, A.M. (2012) Structure of the Alleghanian Thrust Belt Under the Gulf Coastal Plain of Alabama: GCAGS Journal, v. 1, p. 44-54.

Thomas, W.A. (1972) Mississippian Stratigraphy of Alabama: Geological Survey of Alabama Monograph 12, 121 p.

Thomas, W.A. (1976) Evolution of Ouachita-Appalachian Continental Margin: The Journal of Geology, v. 84, p. 323-342.

Thomas, W.A. (1977) Evolution of Appalachian-Ouachita Salients and Recesses From Reentrants and Promontories in the Continental Margin: American Journal of Science, v. 277, p. 1233-1278

Thomas, W.A. (1982) Stratigraphy and structure of the Appalachian fold and thrust belt in Alabama, in Thomas, W.A., and Neathery, T.L. eds., Appalachian thrust belt in Alabama: tectonics and sedimentation: Alabama Geological Society, 13th Annual Field Trip Guidebook, p. 55-66.

Thomas, W.A. (1985a) The Appalachian-Ouachita Connection: Paleozoic Belt at the Southern Margin of North America: Annual Review of Earth and Planetary Sciences, v. 13, p. 175-199

Thomas, W.A (1985b) Northern Alabama sections, *in* Woodward, N.B., ed., Valley and Ridge thrust belt: balanced structural sections, Pennsylvania to Alabama: University of Tennessee Department of Geological Sciences Studies in Geology 12, p. 54-60

Thomas, W.A. (1990) Controls on Locations of Transverse Zones in Thrust Belts: Eclogae Geologicae Helvetiae, v. 83, p. 2166-2178

Thomas, W.A. (1991a) The Appalachian-Ouachita Rifted Margin of Southeastern North America: Geological Society of American Bulletin, v. 103, p.415-431.

Thomas, W.A. (1991b) Tectonic Setting of the Cahaba Synclinorium, *in* Thomas, W.A., and Osborne, W.E., eds., Mississippian-Pennsylvanian Tectonic History of the Cahaba Synclinorium: Alabama Geological Society Guidebook, 28th Annual Field Trip, p. 29-36.

Thomas, W.A. (1995) Diachronous Thrust Loading and Fault Partitioning of the Black Warrior Foreland Basin Within the Alabama Recess of the Late Paleozoic Appalachian-Ouachita Thrust Belt: Society of Economic Paleontologists and Mineralogists Special Publication 52, p. 111-126.

Thomas, W.A. (2001) Mushwad: Ductile Duplex in the Appalachian Thrust Belt in Alabama: AAPG Bulletin, v. 85, p. 1847-1869

Thomas, W.A. (2006) Tectonic Inheritance at a Continental Margin: GSA Today, v. 16, p. 4-11.

Thomas, W.A. (2007) Role of the Birmingham Basement Fault in Thin-Skinned Thrusting of the Birmingham Anticlinorium, Appalachian Thrust Belt in Alabama: American Journal of Science, v. 307, p. 46-62.

Thomas, W.A., Astini, R.A., Osborne, W.E., and Bayona, G. (2000) Tectonic Framework of Deposition of the Conasauga Formation in Osborne, W.E, Thomas, W.A., and Astini, R.A., eds., The Conasauga Formation and Equivalent Units in the Appalachian Thrust Belt in Alabama: Alabama Geological Society, 37th Annual Field Trip Guidebook, p. 19-40.

Thomas, W.A., and Bayona, G. (2005) The Appalachian Thrust Belt in Alabama and Georgia: Thrust-Belt Structure, Basement Structure, and Palinspastic Reconstruction: Geological Survey of Alabama Monograph 16, 48 p.

Thomas, W.A. and Bearce (1969) Sequatchie Anticline in North-Central Alabama, *in* Hooks, W.G., ed., The Appalachian Structural Front in Alabama: Alabama Geological Society Guidebook, 7th Annual Field Trip, p. 26-43.

Thomas, W. A., and Mack, G. H. (1982) Paleogeographic relationship of a Mississippian barrier-island and shelf-bar system (Hartselle Sandstone) in Alabama to the Appalachian-Ouachita orogenic belt: Geological Society of America Bulletin, v. 93, p. 6-19.

Thomas, W.A. and Osborne, W.E. (1995) The Appalachian Thrust Belt in Alabama: Influences on Structural Geometry: Geological Society of America Field Trip Guide Book #9, p. 209-237

Thomas, W. A., and Pashin, J. C., eds., (2011) Of mushwads and mayhem: disharmonically deformed shale in the southern Appalachian thrust belt: Alabama Geological Society 48th Annual Field Trip Guidebook, 126 p.

Tull, J.F. (1982) Stratigraphic framework of the Talladega slate belt, AlabamaAppalachians: Geological Society of America Special Paper 191, p. 3-18.

Viele, G.W. and Thomas, W.A. (1989) Tectonic synthesis of the Ouachita orogenic belt, in Hatcher, R.D., Thomas, W.A., and Viele, G.W., eds., The Appalachian-Ouachita orogen in the United States: Geological Society of America, The Geology of North America, v. F-2, p. 695-728.

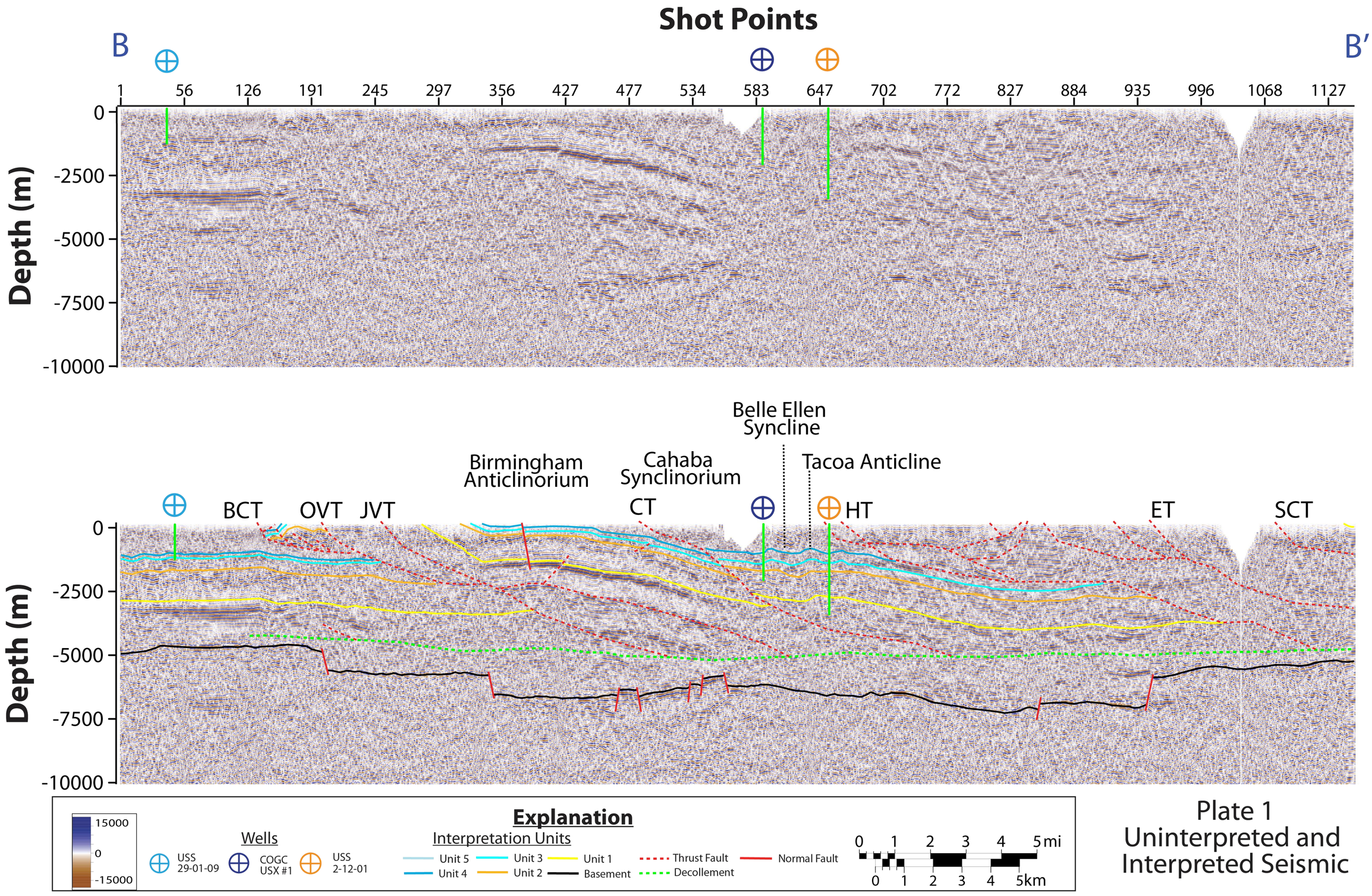

Plate 1
Uninterpreted and
Interpreted Seismic